İSTANBUL TECHNICAL UNIVERSITY ★ INSTITUTE OF SCIENCE AND TECHNOLOGY

ULTRA WIDE BAND SIGE LOW NOISE AMPLIFIER DESIGN

M.Sc. Thesis by
Murat KINALI

Department : **Electronics and Communication Engineering**

Programme : **Electronics Engineering**

JANUARY 2010

İSTANBUL TECHNICAL UNIVERSITY ★ INSTITUTE OF SCIENCE AND TECHNOLOGY

ULTRA WIDE BAND
SIGE LOW NOISE AMPLIFIER DESIGN

M.Sc. Thesis by
Murat KINALI
(504051215)

Date of submission : **25 December 2009**
Date of defence examination: **28 January 2010**

Supervisor (Chairman) : **Prof. Dr. Osman PALAMUTÇUOĞLU (ITU)**
Members of the Examining Committee : **Prof. Dr. Melih PAZARCI (ITU)**
Prof. Dr. Sıddık YARMAN (IU)

JANUARY 2010

<u>İSTANBUL TEKNİK ÜNİVERSİTESİ ★ FEN BİLİMLERİ ENSTİTÜSÜ</u>

ULTRA GENİŞ BANTLI SIGE DÜŞÜK GÜRÜLTÜLÜ KUVVETLENDİRİCİ TASARIMI

YÜKSEK LİSANS TEZİ

Murat KINALI
(504051215)

Tezin Enstitüye Verildiği Tarih : 25 Aralık 2009
Tezin Savunulduğu Tarih : 28 Ocak 2010

Tez Danışmanı : Prof. Dr. Osman PALAMUTÇUOĞLU (İTÜ)
Diğer Jüri Üyeleri : Prof. Dr. Melih PAZARCI (İTÜ)
Prof. Dr. Sıddık YARMAN (İÜ)

OCAK 2010

FOREWORD

First of all, I would like to thank to my supervisor Prof. Dr. Osman PALAMUTÇUOĞLU for his patience and support during my M.Sc. thesis.

I would like to thank to M.Sc. Uğur UYANIK and M.Sc. Başak BASYURT for their kindly support and suggestions. In this point I should open another page for Uğur. As a friend he has been with me since the first days of our undergrad education. I am grateful for his priceless friendship.

I am also grateful to my family for their encouragement and support in every time of my life. I achieved every success in my life with their support. They always believe that I would try to do my best under every condition.

Finally, I would like to thank to all of my friends, relatives and colleagues. Everyone in my life try to help me in thesis period.

January 2010

Murat Kınalı

Electronics Engineer

TABLE OF CONTENTS

Page

ABBREVIATIONS

ADC	: Analog to Digital Converter
AMCC	: Applied Micro Circuits Corporation
AMS	: Austriamicrosystems
BiCMOS	: Bipolar Complementary Metal Oxide Semiconductor
BJT	: Bipolar Junction Transistor
C	: Carbon
CB	: Common Base
CC	: Common Collector
CDMA	: Code Division Multiple Access
CE	: Common Emitter
CG	: Common Gate
CMOS	: Complementary Metal-Oxide Semiconductor
CS	: Common Source
DAC	: Digital to Analog Converter
DoD	: Department of Defense
DS-UWB	: Direct Sequence Ultrawide Band
EIRP	: Effective Isotropic Radiated Power
FFT	: Fast Fourier Transform
GaAs	: Gallium Arsenide
Ge	: Germanium
GHz	: Giga Hertz
GSM	: Global System for Mobile Communications
HBT	: Heterojunction Bipolar Transistor
HD	: High Definition
HEMT	: High Electron Mobility Transistor
HF	: High Frequency
IEEE	: Institute of Electrical and Electronics Engineers
I/O	: Input/Output
InP	: Indium Phosphide
IR	: Impulse Radio
LAN	: Local Area Network
LNA	: Low Noise Amplifier
LOS	: Line of Sight
LPF	: Low Pass Filter
MAN	: Metropolitan Area Network
MB-OFDM	: Multiband Orthogonal Frequency Division Multiplexing
MHz	: Mega Hertz
NLOS	: Non-Line of Sight
PAN	: Personal Area Network
PDA	: Personal Digital Assistant
PLL	: Phase-Locked Loop
RF	: Radio Frequency

RFID : Radio Frequency Identification
R&O : Report and Order
RX : Reception
SAN : Satellite Area Network
SNR : Signal to Noise Ratio
Si : Silicon
SiGe : Silicon-Germanium
TX : Transmission
VCO : Voltage Controlled Oscillator
VLSI : Very Large Scale Integration
USA : United States of America
UWB : Ultra Wide Band
WAN : Wireless Area Network
Wi-Fi : Wireless Fidelity
WiMAX : Worldwide Interoperability for Microwave Access
WLAN : Wireless Local Area Network
WPAN : Wireless Personal Area Network
WWAN : Wireless Wide Area Network

LIST OF TABLES

Page

LIST OF FIGURES

Page

LIST OF SYBOMLS

α	: Common base current gain
BV	: Breakdown voltage
BW	: Band width
β	: Common emitter current gain
γ	: Channel thermal noise coefficient
C_{bc}	: Total base collector capacitance
C_{be}	: Total base emitter capacitance
C_{tc}	: Base and emitter depletion capacitances
C_{te}	: Collector and emitter depletion capacitances
dB	: Decibel
D_{nb}	: Diffusion coefficient of electrons in the base
D_{pe}	: Diffusion coefficient of holes in the emitter
E	: Electric field
E_b	: Band barrier level
E_C	: Energy level of the lower edge of conduction band
E_F	: Fermi level
E_g	: Energy band gap
E_v	: Energy level of the upper edge of valance band
F	: Noise
f_c	: Center frequency
f_{max}	: Maximum oscillation frequency
f_t	: Cut off frequency of a transistor
g_m	: Transconductance of a transistor
I_B	: Base current
I_C	: Collector current
I_E	: Emitter current
J_n	: Electron current density
J_p	: Hole current density
k	: Boltzmann’s constant
L_e	: Total inductance at the emitter of the transistor
C_e	: Total capacitance at the emitter of the transistor including parastics
C_{JC}	: Ease/collector depletion capacitance
C_{JE}	: Emitter/base depletion capacitance
μ	: Mobility
μ_I	: Mobility of impurities
μ_L	: Mobility of influences from lattice vibrations
N_{ab}	: Base doping concentration
N_C	: Effective density of states in the conduction band
N_V	: Effective density of states in the valance band
N_{de}	: Emitter doping concentration
N_{deff}	: Effective doping concentration
NF	: Noise Figure

r	**:** Factor that is related with the temporal width of the pulse
r_b	: Base resistance
r_c	: Dynamic collector resistance
PG	: Processing gain
R_{Load}	: Load resistance
R_n	: Noise resistance
R_O	: Output conductance of a transistor
R_S	: Source resistance
q	: Charge on an electron
τ_B	: Base transit time
T	: Temperature
V_A	: Early voltage
V_{BE}	: Base/emitter voltage
V_{Bias}	: Biasing voltage
V_{CB}	: Base/collector voltage
V_{CE}	: Collector/emitter voltage
v_d	: Drift velocity
v_{sat}	: Saturation velocity
V_{in}	: Input voltage
V_{out}	: Output voltage
W_B	: Basewidth
W_{cb}	: Collector base space–charge region width
Z_{in}	: Input impedance

UWB SIGE LOW NOISE AMPLIFIER DESIGN

SUMMARY

In this work ultra wide technology is investigated. The technological trends in ultra wideband integrated circuit design are examined. The requirements of the technology from the angle of IC designers are expressed. The main purpose of this work is focusing on the design challenges of the low noise amplifiers working on ultra wide band. A new design example in SiGe BICMOS technology is expressed. The performance optimizations for the circuit are considered.

The popularity of wireless standards and the technologies which are developed according to these standards is continuously increasing in telecommunication sector. Wireless telecommunication standards are used in different kind of networks and applications.

Although, Ultra Wide Band (UWB) has been known for a long time, it was standardized in 2002 and started to take place in various high frequency applications. This technology enables high data rates over a wide and free frequency range which lies between 3.1GHz and 10.6GHz.

Low noise amplifier (LNA) is the first block of transreceiver architectures. Low noise amplifier should provide acceptable gain while adding noise as low as possible.

Desigining a low noise amplifier which is working in UWB frquency range has got its own challanges such as having low noise characteristic, low power dissipiation, having 50Ω matching at the input and output and a good linerarty over the whole range.

In this study an Ultra Wide Band low noise amplifier which is working between 1.5GHz and 14GHz is designed in Cadence® Virtuoso Spectre circuit simulator program using 0.35µm SiGe BiCMOS process and the outputs are provided. The proposed amplifier tophology has three stages and 32dB gain.

ULTRA GENİŞ BANTLI SİLİSYUM-GERMANYUM DÜŞÜK GÜRÜLTÜLÜ KUVVETLENDİRİCİ TASARIMI

ÖZET

Bu çalışmada ultra geniş bant teknolojisine yönelik araştırma yapılmış bu konudaki gelişmeler öğrenilmiştir. Bu yeni teknolojiye yönelik tümdevre tasarımına yönelik uygulamalar incelenmiştir. Çalışmanın asıl konusu bu teknoloji ile uyumlu olarak verilen standartlara uygun düşük gürültülü kuvvetlendirici yapılarının incelenmesi ve daha önce SiGe BICMOS teknolojisinde tasarımı ve uygulaması yapılmamış bir devrenin tasarlanarak performans iyileştirmelerinin yapılmasıdır.

Kablosuz ağ standartları ve bu standartlara bağlı olarak ortaya çıkan yeni teknolojilerin telekomünikasyon sektöründeki popülerliği giderek artmaktadır. Kablosuz ağ standartları, veri hızlarına ve band genişliklerine göre değişik kullanım alanlarında ve uygulamalarda yer bulmaktadır.

Ultra Geniş Band (UWB), çok eskiden beri var olan bir teknoloji olmasına rağmen 2002 yılında standartlaşmış ve birçok yüksek frekans uygulamalasında kullanılmaya başlanmıştır. Bu teknoloji 3.1GHz ile 10.6GHz arasını kapsayan ve kullanımı ücretsiz olan geniş bir frekans bandında yüksek hızda veri aktarımına imkan vermektedir.

Yüksek frekans alıcı ve verici yapılarında sistemin ilk bloğu olarak düşük gürültülü kuvvetlendirici hayati bir öneme sahiptir. Düşük gürültülü kuvvetlendiriciden (LNA) çalışılan frekans bandında sisteme olabildiğince az bir gürültü eklerken kabul edilebilir bir düzeyde kazanç sağlamalıdır.

Ultra Geniş Band standartının ortaya koyduğu tasarım ölçülerine sahip bir düşük gürültülü kuvvetlendirici tasarlamanın kendine özgü zorlukları vardır. Kuvvetlendiricinin var olan frekans bandında düşük gürültü karakterstiğine sahip olması, giriş ve çıkış direncinin 50Ω'a eşlenmesi, doğrusallığının iyi olması ve düşük güç sarfetmesi gerçekleştirilmesi gereken tasarım şartlarıdır.

Bu çalışmada UWB frekans bandını da içine alacak şekilde 1.5GHz ile 14GHz frekans aralığında çalışacak düşük gürültülü bir kuvvetlendiri 0.35µm SiGe BiCMOS teknolojisi kullanılarak Cadence® Virtuoso Spectre devre benzetim programında tasarlanmış ve sonuçlar sunulmuştur. Önerilen kuvvetlendirici mimarisi 3 kattan oluşmakta ve 32dB kazanç sağlamaktadır.

1. INTRODUCTION

Telecommunications industry has been one of the key industries since previous centuries. It is leading the electronics and the other related technologies and brings new considerations. From the global view, telecommunication business and its technology have big impacts on the world's politics and economics. In micro level, they affect people' daily lives, human relationships, working disciplines, research areas etc. The combination of telecom companies, vendors, third parties, research and development centres appear as the biggest sector in all developed and developing countries. Every new improvement reaches all over to the world in a short time even to the underdeveloped regions.

In today's telecommunication technology, wireless applications become very popular. The demands of the market increase from day to day. The aim of replacing copper and fibre optics lines between fixed destinations is achieved with the implementation of new standards and technologies. Digital cellular systems, Bluetooth, Wi-Fi, third generation GSM services, Wimax and the forth generation systems preserved the consumer use successively. These technologies enable the consumers can access to the every kind of information from any place and in any time.

As the demands of mankind do not stop the aim of faster, more qualified and more secure service with higher capacity is always kept. Hence, coming out of the new enhanced technologies never stop. In this point the allocation problem of these new standards in the crowded Radio Frequency Spectrum appears. New services bring more detailed and absolute constraints in order prevent interfaces between the new and the existing services in the spectrum.

Ultra-wideband (UWB) technology promises to provide new services as keeping the existence of the current ones without an interference problem. This new technology brings a new standard for wireless communications with its strict rules. The exiting technologies need to be paid expensive fees by providers as they allocate different frequencies of the spectrum. But UWB gives the chance of avoiding these huge costs to the providers as it is working the old standards at the same time without any significant problem.

As the telecommunication technology leads the radio frequency integrated circuit design the ultra-wide band transreceivers are started to be designed. From the RF IC designers' corner, this technology brings new design challenges against its superior advantages.

Low noise amplifier is the vital block of a transreceiver. Thus, it has got its own natural design difficulties which show themselves as ineluctable trade offs between the criterias for the performance. As the transreceiver have to follow the standards of the authorized corporations, LNA design becomes more difficult. The stringent specs determined by ultra-wideband technology makes the designs more critical. On the other hand, this leads to engineers to suggest new approaches and apply new techniques in the design of LNAs for UWB applications.

In this work an UWB LNA design approach is going to be analysed. The outputs are going to be investigated.

The next chapter presents UWB concepts and the historical background of this technology. Its advantages over the current standards are expressed. The chapter continue with two approaches to UWB and it finishes with the newly expressed standards employing UWB requirements.

Silicon-Germanium Heterojunction Bipolar transistors, their operating principles and technological background are the subjects of the third chapter.

In the forth chapter ultra wide LNA design challenges and the ic design solutions to adapt this new standard are presented. The state of art UWB LNA is designed and optimised in SiGe technology which is the goal of this project.

2. ULTRA WIDE BAND TECHNOLOGY

In this chapter, the Ultra-wideband concept is explained and some historical information is given. Current standards and their effects are discussed.

2.1 Wireless Networks

The wireless networks continue to grow and enter the inside of homes, buildings, metropolitan areas as wireless local area networks (WLANs). WLANs also can operate in conjunction with the local area networks (LANs). Two or more LANs come together and form a wide area network (WAN). If the WAN is build up on the wireless radio connection, it is called wireless wide area network (WWAN). Wireless service carriers provide the wireless network structure and make the WWAN spreads often over the whole country. In addition, there are the MAN and the SAN terms, which mean metropolitan area network and satellite area network respectively. Figure 2.1 shows these world communication technologies classified according to their data rates and their usages [1].

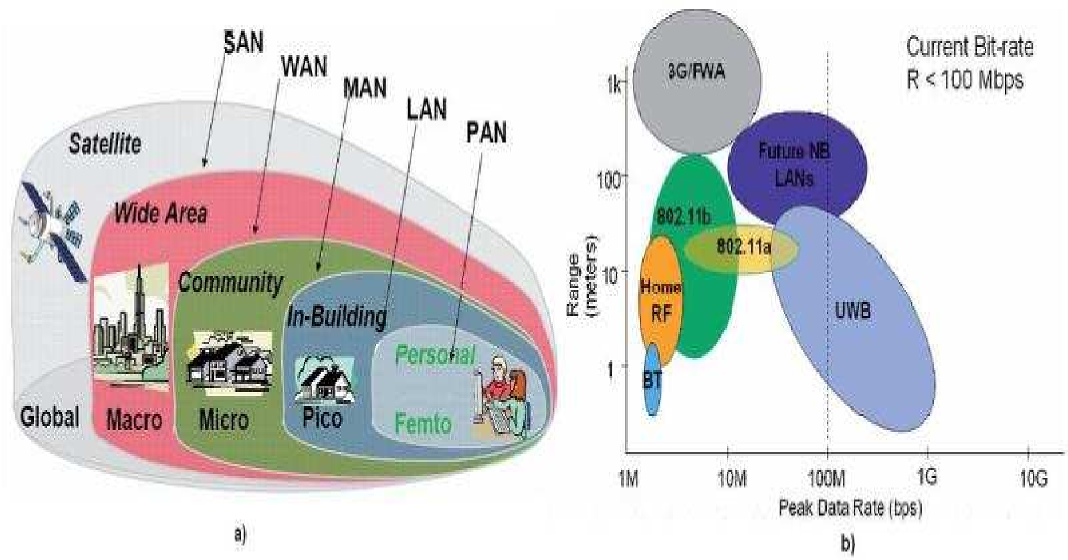

Figure 2.1 : a) Telecommunications technologies' world. b) bit-rates.

Another technology, wireless personal area network (WPAN) is used for high-data rate communication within the very limited distances especially among the consumer electronic devices. WPAN is effective generally for the distances less than seven meters. This limits the devices that can use WPAN, but still there are plenty of different electronic goods such as PDAs, cell phones, pagers, portable computing devices, PCs, game consoles. WPAN makes communication between users of these devices available. More than the communication, simultaneous work is achieved as another great benefit. All of these devices have got same basic attitudes that WPAN brings; low-cost, low-power communication with small compact designs.

Ultra Wide Band takes place in the border of WLAN technology by its principle of high rate data transfer in a short-range [1-4].

2.2 Ultra Wideband Basics

UWB (Ultra Wide Band) is a kind of wireless transmission technology, which gives a great opportunity to transmit huge amount of data over a wide frequency spectrum for short distances using very low power. UWB is also known as digital pulse wireless and it is clear that it has remarkable attributes such as high data rates, ranging and miscellaneous communication applications, reduction of costs and exemption to the multipath fading [1-4].

Taking the telecommunication theory as consideration can be show a meaningful explanation for the usage of UWB. UWB can operate in power limited regime. This can be proven by Shannon's Theorem [2].

$$C = BW \cdot \log\left(1 + SNR\right) \quad \textbf{(2.1)}$$

C is the maximum channel capacity in bit/second, while BW is bandwidth and SNR is the signal to noise ratio. Both terms are directly proportional with C. Increasing both of them increases the channel capacity. But increasing SNR does not provide a low power solution. It is also limited by other terms. Under the limited specs for power, changing the value of the band width is the unique solution for high – data rate communication.

2.3 The History of UWB

There are numerous differences between the principles of the Ultra Wide Band communication and the other communication techniques, because it uses very narrow RF pulses for communication between transmitters and receivers. As performing direct communications based on the short duration pulses, a very wide bandwidth is formed which brings several advantages. Throughput, covertness, robustness to jamming and coexistence with radio service are some advantages that can be expressed at first [1, 4].

UWB becomes very popular recently. The trends on telecommunication sector point ultra wide band but in fact this is not a new technology. Gugliermo Marconi was the first person who used it, in order to transmit Morse code sequences across the Atlantic Ocean via spark gap radio transmitters in 1901. However, the world did not know the benefits of the large bandwidth. Also the capability of the electromagnetic pulses for the purpose of multiuser systems implementation was not noticed.

World waited nearly fifty years to see the usage of UWB in military applications. The research focused on impulsive radars that employed modern pulse-based transmission. Henning Harmuth of Catholic University of America and Gerald Ross and K. W. Robins of Sperry Rand Corporation are some examples for the pioneers of modern UWB communications in the United States from the late 1960s. Between 1960 and 1990 military and Department of Defense (DoD) applications owned the usage of this technology under classified programs such as highly secure communications. With the rapid advancement in semiconductor technology UWB appeared as a solution for commercial applications. By the early 1970s the basic designs for UWB signal systems were available and there remained no major obstacle to progress in perfecting such systems. After the 1970s, the only innovations in the UWB field could come from improvements in particular instantiations of subsystems, but not in the system concept itself. Hence, UWB is the declaration of a long-existing technology with a new name [5].

Several years ago, the world started to interest on UWB as commercial way. The UWB system developers started show their pleasure to the FCC which finally resulted as the approval of UWB for the commercial use. FCC published the First Report and Order (R&O) for commercial use of UWB technology under strict power emission limits for various devices in February 2002. Figure 2.2 illustrates a timeline for the development of UWB.

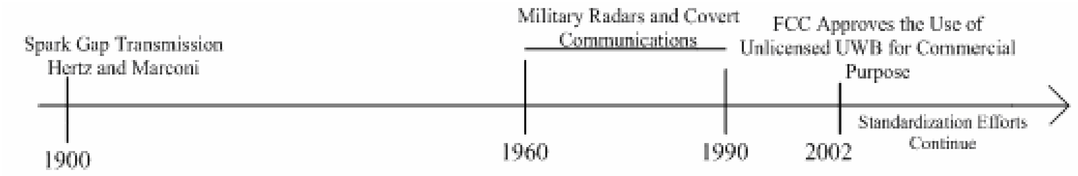

Figure 2.2 : Development timeline of UWB.

Today UWB appears in a wide range of interesting wireless applications. Military usage includes warfare systems for terrestrial and maritime. The commercial applications group includes sensor networks, medical applications, RFID, consumer electronics, adhoc networks, locationing [6].

Individual sensor nodes which are placed in a specific area, come together and form wireless sensor networks. The sensors are used to keep some physical quantities in the environment (e.g. temperature, humidity, position, speed, motion, etc.) in the environment. Wireless sensor networks cannot ignore UWB, because of its small, low power devices that combine location sensing and wireless communication capabilities. The UWB transceivers and antennas can be very small, low power and low cost. Therefore, there are expectations that wireless sensor networking could likely be one of the largest markets for the UWB [6].

Human body can be monitored by electromagnetic UWB pulses. Short duration UWB signals benefits from the difference of reflection indices of the organs and tissue and give their clear pictures. This body monitoring can be done remotely, which is vital for the hygiene of the environment and the mental health of the patients. Moreover, the low power nature of these signals is safe for human body [6].

Radio Frequency Identification (RFID) is an automatic identification technology. Its usage is similar to barcode but it communicates using radio waves. UWB brings an excellent solution for RFID applications because it can provide good connectivity as well as accurate position identification capability. The UWB RFID tags and tag readers can be small and of low-cost [6].

Since UWB offers short-range high-data rate communication, it is very attractive for consumer electronics, such as PCs, game consoles, digital TVs and PDAs etc. wireless high-speed data transmission between DVD players/recorders and (HD) TV and computers is one example for this kind of applications. This technology eliminates the need for cable connection among consumer electronics devices and subsequently increases the freedom and movement of the user [1-3, 6].

An ad-hoc network is a kind of local area network (LAN) that is built spontaneously as devices connect. There is no need to set a base station in these networks. Instead, the nodes forward packets to and from each other by their selves**.** Similaryly, in wireless ad hoc networks each mobile can act as a terminal and as a router. UWB technology is an interesting and new opportunity for the wireless ad hoc networks because it is a possible solution for the design challenges; the location of mobile, the constraint on power consumption of battery-powered mobile terminals and multipath [6].

One of the technological preferences is UWB for identification of location. The precise location measurement and its usage in the asset management is an important application of the UWB technology. Market researches show that there will be significant market in the coming years. Also, the location capability can also be used to locate personnel, inventory items, and vehicular robots in indoor environments [6].

2.4 UWB Signals

The existing narrowband communications systems modulate continuous-waveform radio frequency signals with a specific carrier frequency to transmit and receive information. A continuous-waveform has been placed in a narrow frequency band with a well definition. This makes it unprotected against to detection and interception. Figure 2.3 and Figure 2.4 shows a narrowband signal in the time and frequency domains respectively [3]:

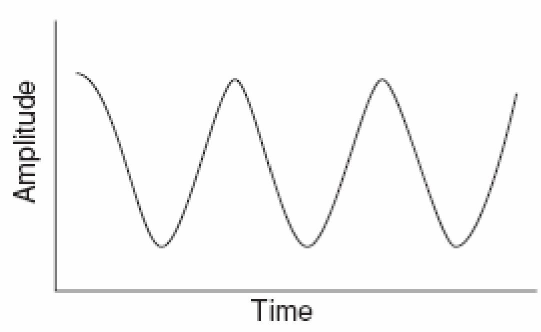

Figure 2.3 : Narrow band Signal in the time domain.

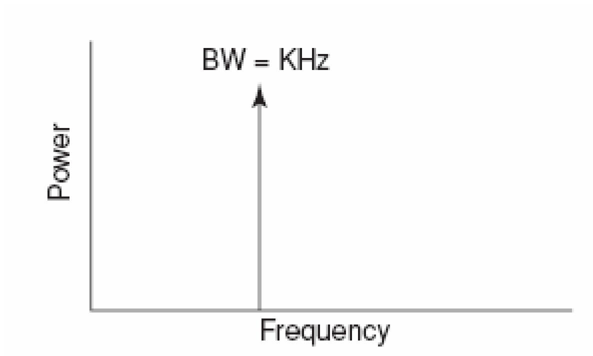

Figure 2.4 : Narrow band Signal in the frequency domain.

UWB systems employ carrierless, short-duration (maximum in nanoseconds) pulses having a very low duty cycle (it less than 0.5 percent) in transmitting and receiving data. The ratio between the time of the pulse's presentation and the total transmission time is called as duty cycle. Figure 2.5 shows it clearly [3].

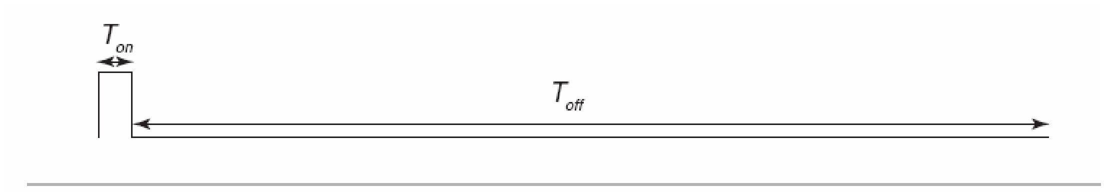

Figure 2.5 : Pulse having low duty cycle.

The signal exists during T_{on} and it is transmitted in T_{off}. The signal is not present while T_{off}. According to its description duty cycle can be formulated as:

$$\text{Duty cycle} = \frac{T_{on}}{T_{on} + T_{off}} \qquad \textbf{(2.2)}$$

Low duty cycle provides a very low average transmission power which is defined in microwatts in ultra-wideband communications systems. Although the maximum power level of individual pulses might be relatively large as they are present in a time shorter than a nanosecond, the average power becomes very low. As the technology takes places in handheld systems low transmit power requirement means longer battery life. Hence time and frequency have inverse relation, the short, duration UWB pulses keep their energy across a wide frequency range between nearly DC to several gigahertz with very low power spectral density. Power spectral density is the power of the signals in the frequency domain [3].

$$PSD = \frac{P}{BW} \tag{2.3}$$

In (2.3) P is the power transmitted in Watts (W), BW is the bandwidth of the signal in Hertz (Hz) and the PSD is in unit of W/Hz.

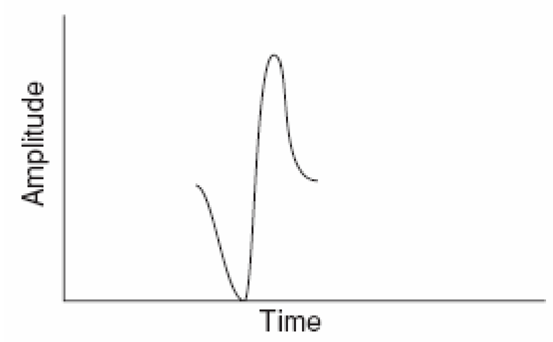

Figure 2.6 : UWB Signal in the time domain.

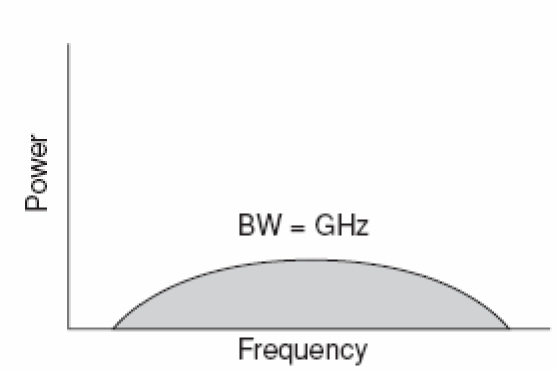

Figure 2.7 : UWB Signal in the frequency domain.

Figures 2.6 and 2.7 are the illustrations for the time and frequency behavior of the UWB Signals respectively.

Fourier transforms can give instantaneous bandwidth results theoretically with the time scaling property [3].

$$x(at) \longleftrightarrow \frac{1}{|a|} X\left(\frac{f}{a}\right) \tag{2.4}$$

In (2.4) left side presents a single in the time domain as the right side presents it in the frequency domain. x(t) is scaled in the time domain by the factor a while the x(f) scaled by 1/a. Think about a pulse with 400ps duration. It can achieve a center frequency (f_c) 2,5GHz.

$$f_c = \frac{1}{T} = \frac{1}{400 \cdot 10^{-12}} = 2,5 \cdot 10^9 H = 2,5GHz \tag{2.5}$$

In that point the signals have to compatible with the FCC's First Report and Order in order to be classified as UWB signals. FCC defines the UWB as any wireless structure that uses either a fractional bandwidth of $BW/f_c > 20\%$ where BW is the operating bandwidth and f_c is the center frequency of the operating band. FCC accepts another definition, which states that f_c is more than 500MHz of absolute bandwidth. The fractional bandwidth is a useful term to describe the signals as narrowband, wideband and ultra-wideband. The FCC's first definition is based on this term too. It is the ratio of bandwidth at the points, which are in the 10dB neighborhood of the center frequency. The 10dB neighborhood represents a range in which the spectral power of signal is 10dB lower than the maximum power.

$$B_f = \frac{BW}{f_c} \times 100\% = \frac{(f_h - f_l)}{(f_h + f_l)/2} \times 100\% = \frac{2(f_h - f_l)}{(f_h + f_l)} \times 100\% \tag{2.6}$$

(2.6) formulates the definition where the f_h and f_l are the highest and lowest cut off frequencies at the 10dB points of the UWB frequency range. A UWB signal can be in the form of one kind of the wideband signals such as Gaussian, chirp, wavelet or Hermit-based short duration pulses. Gaussian based UWB pulse is demonstrated in Figure 2.8 and Figure 2.9. The signal can be defined as (2.7) [3]

$$h(t) = 6A\sqrt{\frac{e\pi}{3}}\frac{t}{1/f_c}e^{-6\pi(t.f_c)^2} \tag{2.7}$$

where t is the time and A is amplitude scaling factor. The pulse with the 500ps duration forms a large bandwidth with 2GHz centre frequency in the Figures 2.8. The values of the f_h and f_l are seen on the Figures 2.9 as 1.2GHz and 2.8GHz which give the B_f as %80 in (2.8).

$$B_f = 2 \times \frac{(2,8 - 1,2)}{(2,8 + 1,2)} \times 100\% = 80\% \tag{2.8}$$

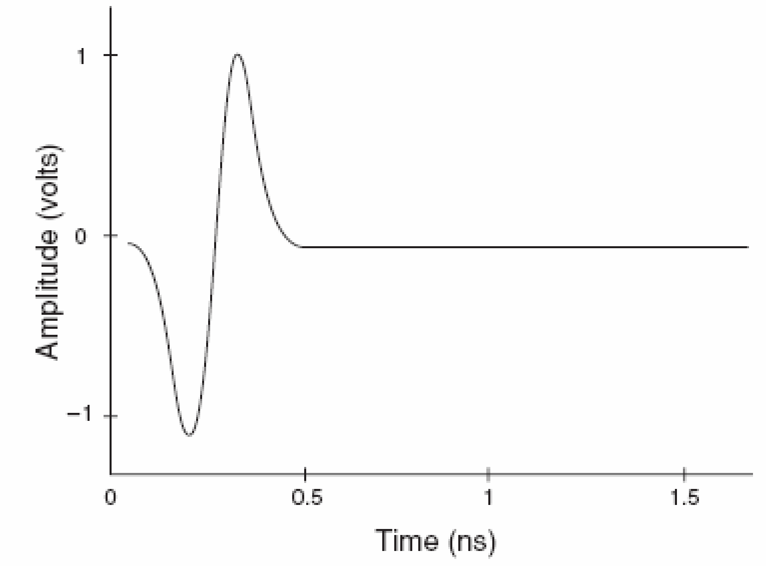

Figure 2.8 : A Gaussian monocycle in the time domain.

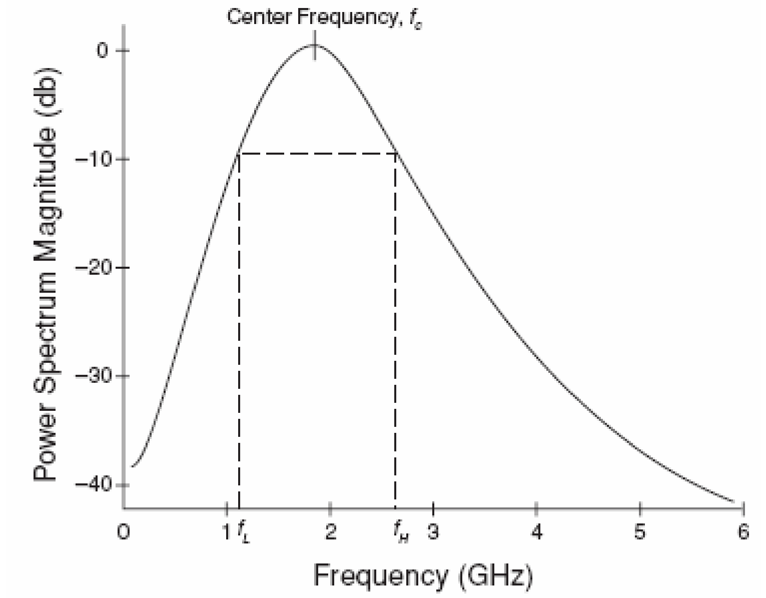

Figure 2.9 : A Gaussian monocycle in the frequency domain.

80% B_f is a huge value as the 20% fractional bandwidth is enough for a signal to be defined as UWB. Table 2.1 gives an idea for the classification of the signals according to their fractional bandwidths [3].

To give an example Bluetooth signals which are well known for the consumers described as narrowband signals with their 0,04% B_f.

Table 2.1: The classification of the signals with fractional bandwidth

Narrowband Signals	$B_f < 1\%$
Wideband Signals	$1\% < B_f < 20\%$
UWB Signals	$20\% < B_f$

2.5 Characteristic of the UWB

UWB is a wireless radio technology that enables the high speed data transfer and location determining applications. Its attractiveness for the consumer applications comes from its features such as

- having potentially low complexity and low cost
- having noise-like signal spectrum
- being resistant to severe multipath and jamming
- having very good time-domain resolution allowing for location and tracking applications.

The UWB signals' transmission is not very different from the narrowband signals'. This brings low complexity and low cost. Because of the nature of these signals as described under the previous title the UWB receivers do not need additional up-conversion and down-conversion because of their well propagation as they span the common carrier frequencies. This removes RF Mixing stage that means there is no need to the local oscillator and phase tracking loops. Thus UWB based radio frequency integrated circuits do not need high power and high costs.

In consequence of low power density and pseudo-random characteristics of the transmitted UWB signals they are noise-like signals as seen in the Figure 2.10.

Without deliberation they cannot be detected easily. More important than this interference problems with the current radio systems are kept in minimum level.

Multipath fading occurs when a transmitted signal divides and takes more than one path to the receiver and some of the signals arrive out of phase. This causes weaker or fading signal. As various surfaces like trees, buildings and people provides extra reflections to the transmitted signal the multipath is unavoidable in communication systems. The multipath is described in the Figure 2.11.

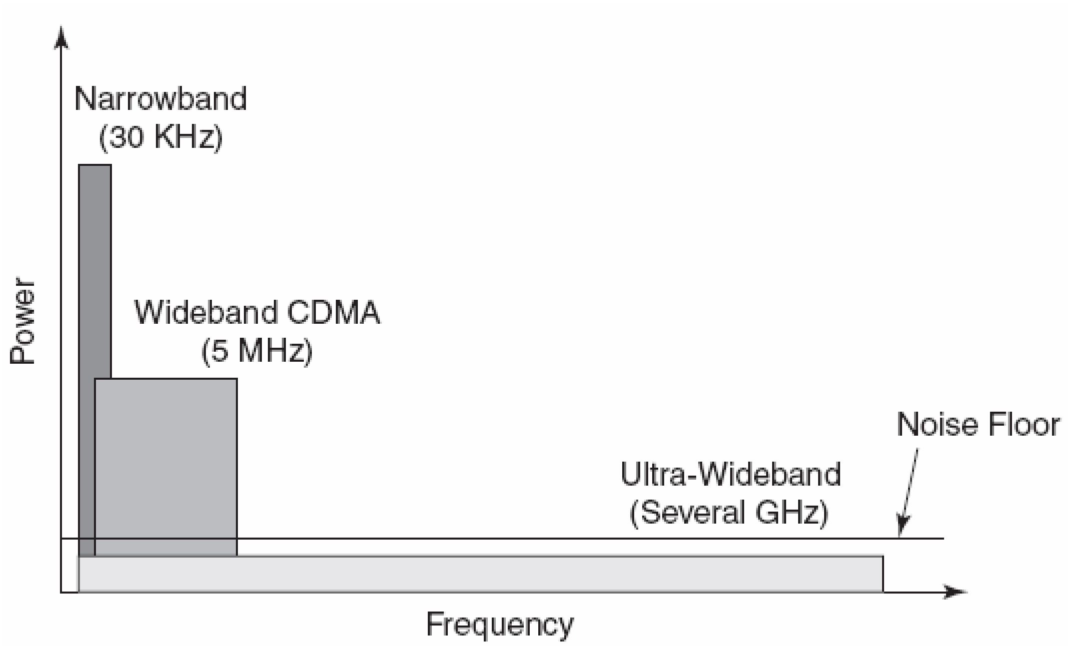

Figure 2.10 : Coexistence of UWB signals with other signals.

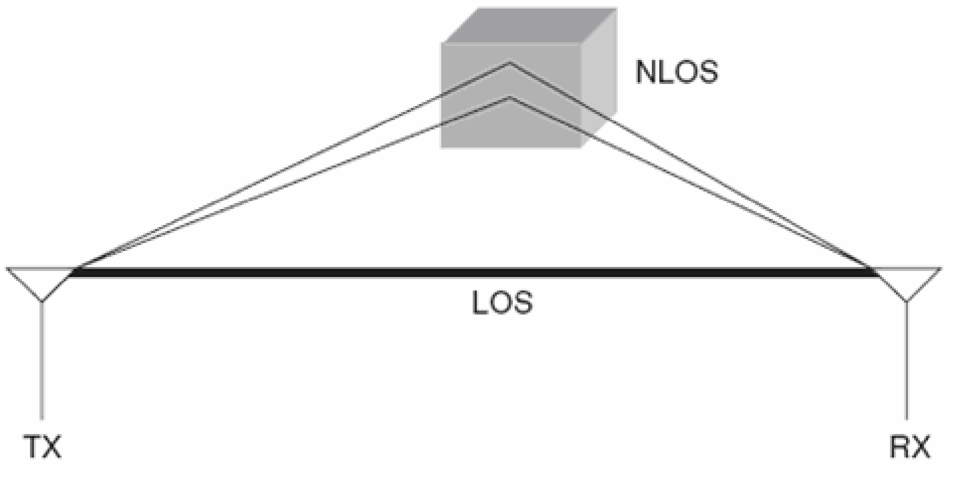

Figure 2.11 : The multipath in wireless communication channels.

The LOS corresponds to the line of sight which is the straight way between transmitter and the receiver. The NLOS, non-line of sight is the unwanted way between the transmitter and the receiver as mentioned above. Having deep impacts on the narrowband systems multipath is a fatal problem as seen clearly in Figure 2.12.

In UWB, the transmitted signal's bandwidth is very large which leads to significant resolution. Discrete transmission and the huge frequency diversity make these signals strong to multipath propagation (seen on the Figure 2.13) and also jamming. Comparing the situations between the Figure 2.12 and Figure 2.13 proves the severity of the problem in narrowband systems is higher. The sensitivity of the UWB signals against to the multipath fading is low because of their short duration characteristic.

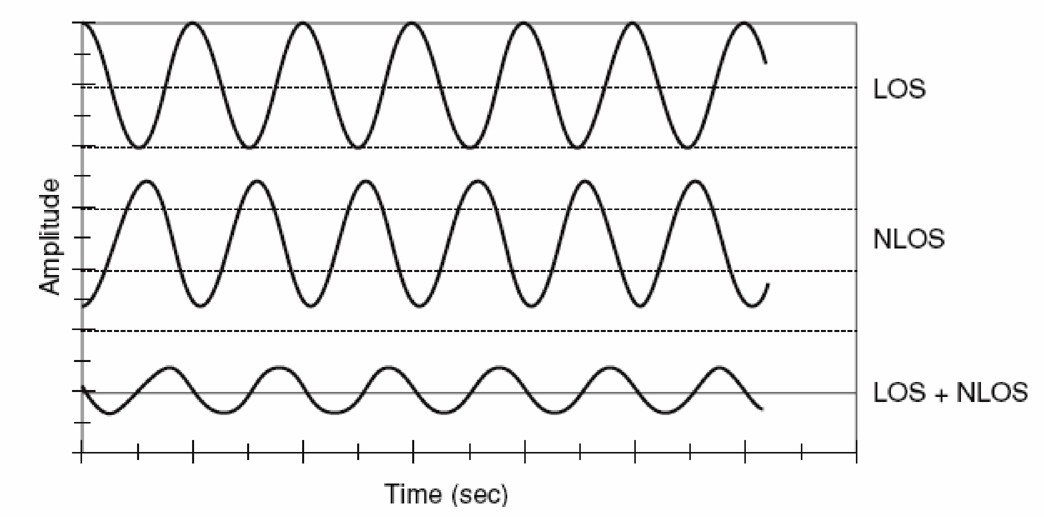

Figure 2.12 : The multipath problem for narrowband signals.

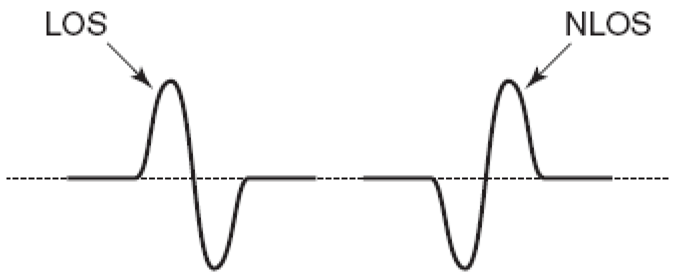

Figure 2.13 : The effects of Multipath on UWB signals.

On the other hand, no jammers can jam in every frequency in this very large frequency range. UWB systems preserve good low probability of interception and low probability of detection. These features make the UWB useful and efficient for military projects. Theoretically this can be explained by (2.9):

$$PG = \frac{RF\ Bandwidth}{Information\ Bandwidth} \tag{2.9}$$

PG is the processing gain which is a measure of radio system strength against to jamming. The huge frequency diversity is the result of the high PG in UWB systems.

UWB communication systems bring very effective solution to transmit high data rates. Hundreds of Mbps data rates are valid levels in this technology as well as the low rates.

Finally there is one more vital advantage with this technology. These systems are suitable for short-range radar applications as they are capable to pass into materials like walls and they have good timing precision. This vital advantage gives the chance to these systems to take place in rescue and security operations, surveying and mining as well as the consumer wireless communications. But this advantage is effective in only the low frequency region of the RF spectrum. It means that targeting and the penetration are not in high quality at the same time.

2.6 The Standardization of UWB and Regulations

As mentioned under the previous titles FCC put a clear definition to UWB with the First Report and Order in February 2002. The UWB systems have to be compatible with its determined concepts. FCC defines the UWB as any wireless structure that uses either a fractional bandwidth of $BW/f_c > 20\%$ where BW is the operating band width and f_c is the center frequency of the operating band. FCC accepts another definition which states that f_c is more than 500MHz of absolute bandwidth. The frequency range is determined as 7.5GHz between the 3.1GHz and 10.6GHz frequencies with limited transmit power of -41.3dBm/MHz or 75nW/MHz is allowed for UWB radio usage as unlicensed. Figure 2.14 shows the exact limits [2, 5-7]. A pulse signal which is centred at 6GHz and occupies a bandwidth of more than 1.2GHz can be given as an example for UWB pulses [1-7].

The rules of FCC are very strict and put different values as the dividing the UWB devices into three classes. Table 2.2 shows the classes and the emission limits.

On the other hand, UWB regulation standards are formulated based on local needs. The emission limit in Korea is lower than the FCC level while it is 6dB higher in Singapore. Although the limitations are similar with FCC, the outdoor usage of UWB has not been allowed so far in Japan [6].

These restrictions on the transmit power, PANs and sensor networks are more suitable for UWB communications as they are kinds of short-range communication.

IEEE 802.15 initiative works on development of standards for Wireless Personal area Networks (WPAN) or short range networks. 802.15.1 has brought a WPAN standard based on Bluetooth. In order to enable the coexistence of WPAN (802.15) with WLAN (802.11), the 802.15.2 was developed [6].

Table 2.2: Emission Limits for UWB Devices (ERIP in dBm) [5].

Operation Band (GHz)	Application			
	Indoor Communication	Outdoor Communication	Imaging	Vehicular Radar
0.96-1.61	-75.3	-75.3	-53.3	-75.3
1.61-1.99	-53.3	-63.3	-51.3	-63.3
1.99-3.1	-51.3	-61.3	-41.3	-63.3
3.1-10.6	-41.3	-41.3	-41.3	-63.3
10.6-22.0	-51.3	-61.3	-41.3	-41.3
22.0-29.0	-51.3	-61.3	-51.3	-41.3

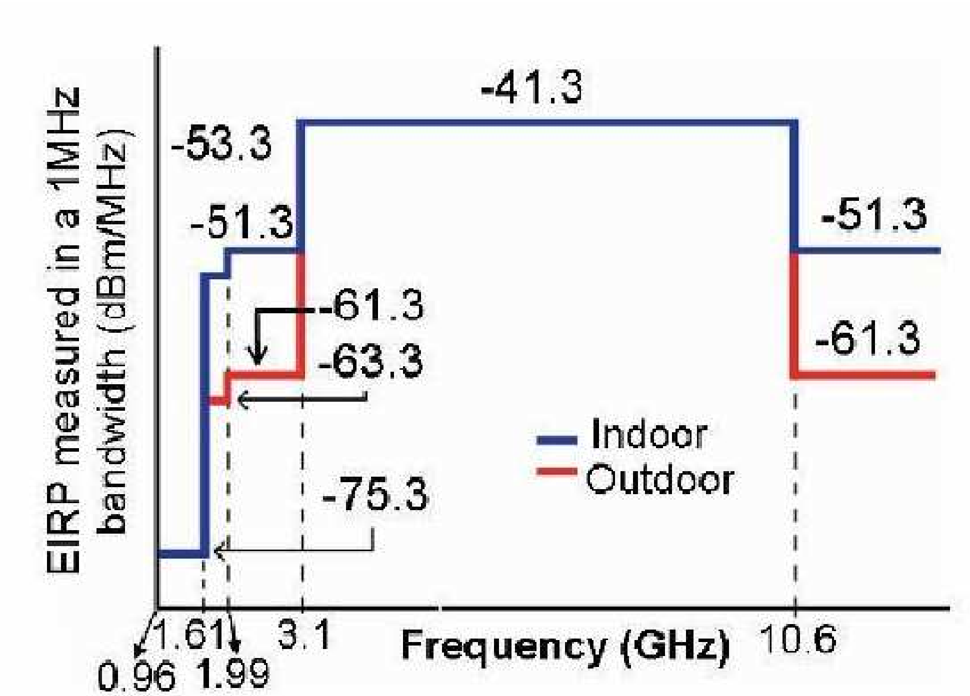

Figure 2.14 : FCC limits for transmitted power and UWB spectral mask.

IEEE established a group for standardization purpose inside 802.15.3. Because of this concentration, IEEE 802.15.3a was developed for UWB PANs [7-8]. The new standard enables higher data rates up to 110Mb/s at 10m distance and 200Mb/s at 4m distance. This data rates are going higher and higher as the distance gets smaller. The table 2.3 shows a summary for this standard.

The IEEE 802.15.4 Zigbee is a different block of standards which investigates a low data rate solution with multi-month to multi-year battery life and very low complexity [6].

Table 2.3: IEEE 802.15.3a summary requirements [7]

Parameter	**Values**
Bit Rate	110, 220, 480Mbps
Range	30ft, 12ft
Power consumption	100mW, 250mW
Bit Error Rate	1E-5
Co-located piconets	4
Interference capability	Robust to IEEE Systems
Co-existence capability	Reduced interference to IEEE Systems

Recently there are two approaches are accepted in UWB as FCC lost the definition of UWB [8].

2.6.1 Direct sequence UWB (DS-UWB) proposal

In DS-UWB there are two independent bands for operation. The lower band allocates the spectrum from 3.1 GHz to 4.85 GHz and the upper band allocates the spectrum from 6.2 GHz to 9.7 GHz.

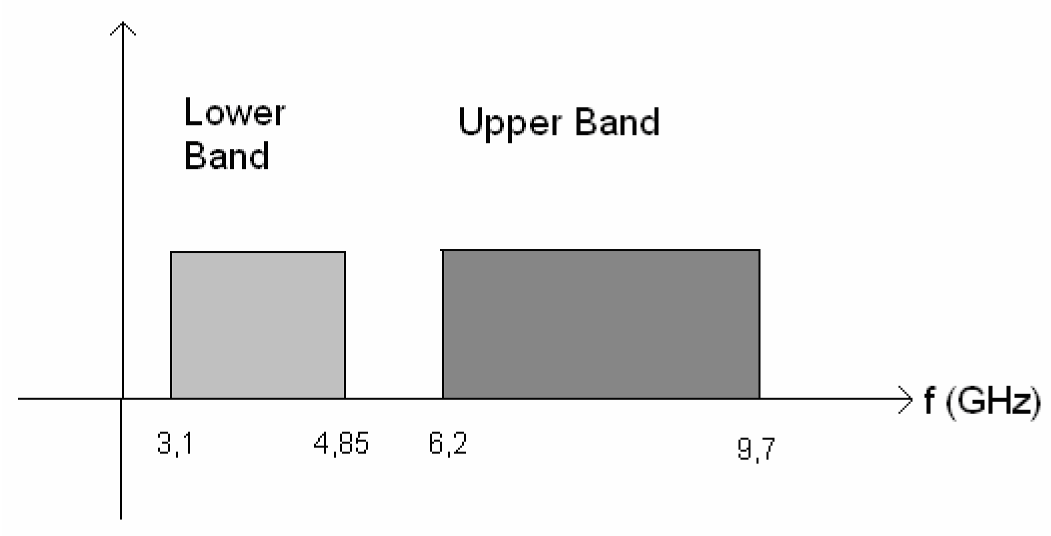

Figure 2.15 : DS-UWB sub-bands [9].

2.6.2 Multiband Orthogonal Frequency Division Multiplexing UWB

This proposal divides the UWB into five main sub-bands. Inside these sub-bands there are 14 sub-bands with the bandwidth of 528MHz [2].

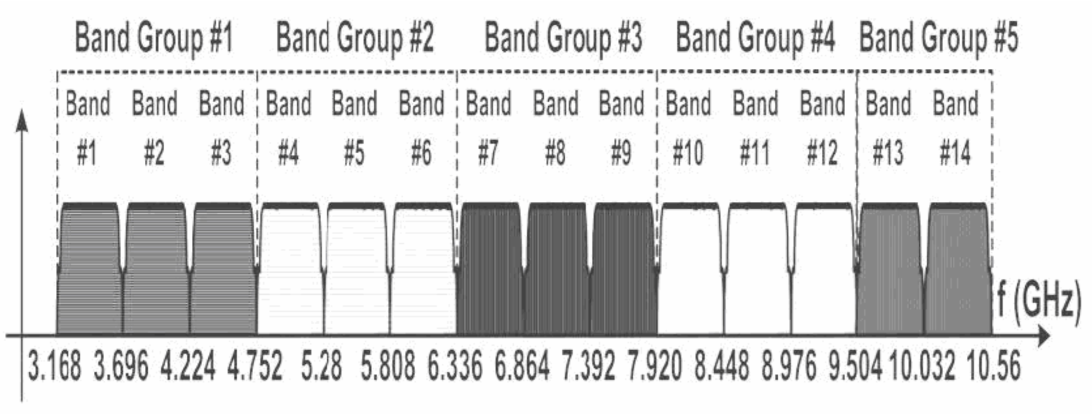

Figure 2.16 : MB-OFDM UWB sub-bands [9].

Both of the proposals are technically valid and impressive. Supporters of DS-UWB criticize the MB-OFDM systems for their complexity, which results from using complex Fast Fourier Transforms (FFTs). On the other side, supporters of multiband OFDM believe that their technique offers better coexistence with other radio services, and they disapprove of DS-UWB because of possible interference concerns.

2.7 UWB Integrated Circuit Design

As the UWB becomes very popular in telecommunication industry and starts taking place in applications the demands from the microelectronics industry get higher. The designers answered this demand by focusing UWB integrated circuit design. Working on a new and a popular technology is very attractive but it is obvious that designing radio frequency integrated circuits for ultra wide band technology brings great challenges. Firstly, using CMOS devices for the low cost implementations increases the challenges. The stringent requirements of the specs are great obstacles that appear on the design period. The large frequency gap states that the UWB transreceivers containing low noise amplifiers (LNAs), mixers, correlators should be able to work with very wide bandwidth signals spread over wide range of frequencies. The circuits have to show the characteristics such as gain, noise figure and linearity between 3.1 – 10.6GHz. Under a power limit satisfying these conditions is the key issue for designers [9-11].

An extra design challenge is the sensitivity of the low Q systems against to the parasitics, especially in pads and wire bonds, is very high. Receiver architectures require good isolation among subbands. Also the transition from one subband to another should be very quick. Fast switching is another key issue in UWB design.

For the wireless applications the UWB technology has got effects on transreceiver architectures. There are two common transreceiver types working according to this standard.

2.7.1 Impulse radio UWB receiver

The IR-UWB based on technology without carrier which yields the transmission of the signal from antenna to the air directly. Thus, the necessity of the complex frequency blocks is over. This is a definite difference from narrow band receivers. The low power emission must turns into an advantage in the transmitters' antenna pre-drivers by making the design easier. This is also a big difference from narrow-band receivers [1].

Figure 2.17 illustrates the IR-UWB Receiver blog diagram. Replacing an analog correlator after LNA sends the ADC further part of the chain which causes the decrease in the performance requirement of the ADC.

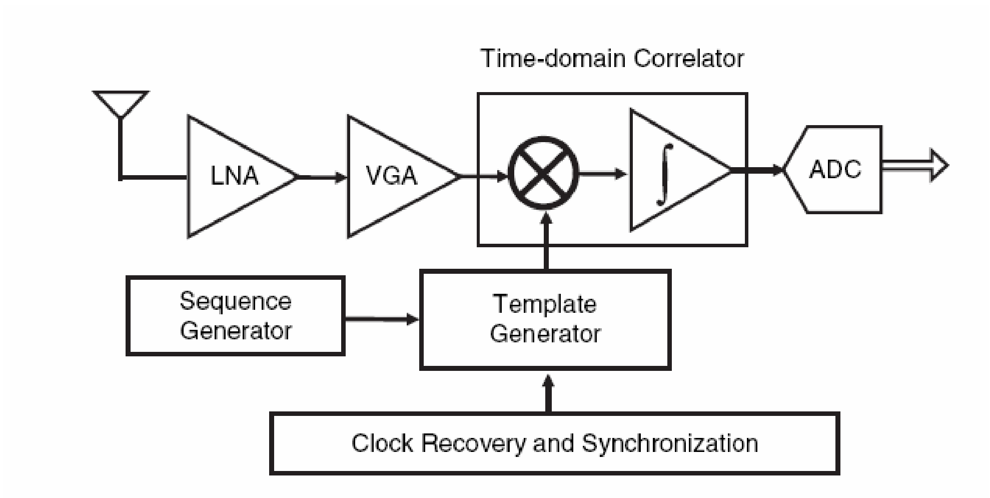

Figure 2.17 : Impulse radio UWB receiver.

2.7.2 MB-OFDM UWB receiver

High data rates can be transmitted by using relatively cheap receivers. Figure 2.18 illustrates the block diagram of these kind UWB receivers. The pre-select filter which is placed just after the antenna blocks the out-of-band noise and only passes the desired band UWB Signal. The received ultra-wideband signal is amplified and down-converted by the LNA and he mixers. The low-pass filter and VGA make the signal ready to ADC as filtering the out-of-band signals and setting the required amplitude. The received baseband signals are used for FFT operation at the final step by the digital signal processing unit [1].

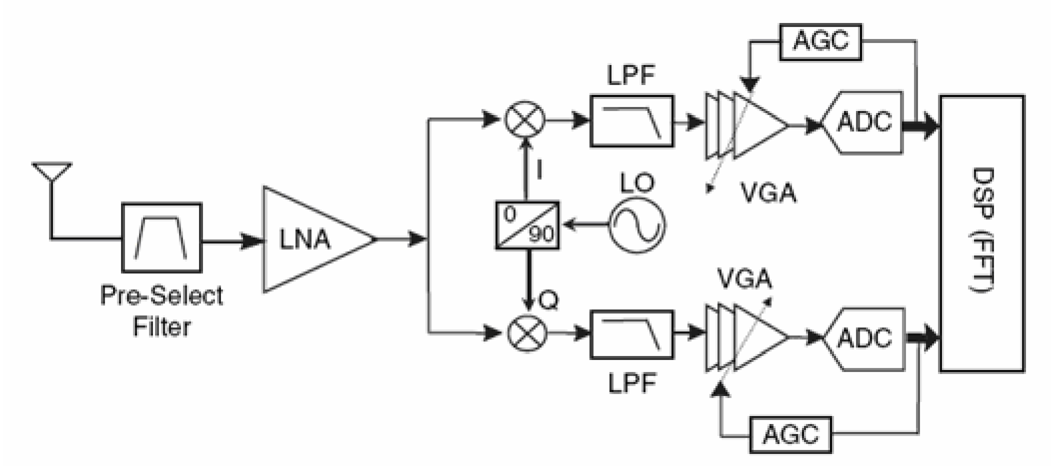

Figure 2.18 : MB-OFDM UWB receiver [1].

2.7.3 Ultra-bad vs. narrowband

As examined previous sections, the narrowband and ultra-wideband transreceivers are having different architectures as illustrated in Figure 2.19.

Not only the architectures the antenna, front-end, analog and digital baseband need to be compared. Looses of power-efficient antennas, pulse shape distortions, ringing due to the filter characteristics of antenna and the communication channel, wideband matching and power consumption of low noise amplifier are major challenges in UWB designing Baseband design causes the another challenge. As the short length pulses are employed in UWB communications the high resolution must which increases the acquisition time and requires extra correlators appears. Digital technology choices lead to the requirement of fast ADCs with huge number of correlators. Table 2.4 summarizes the considerations [11].

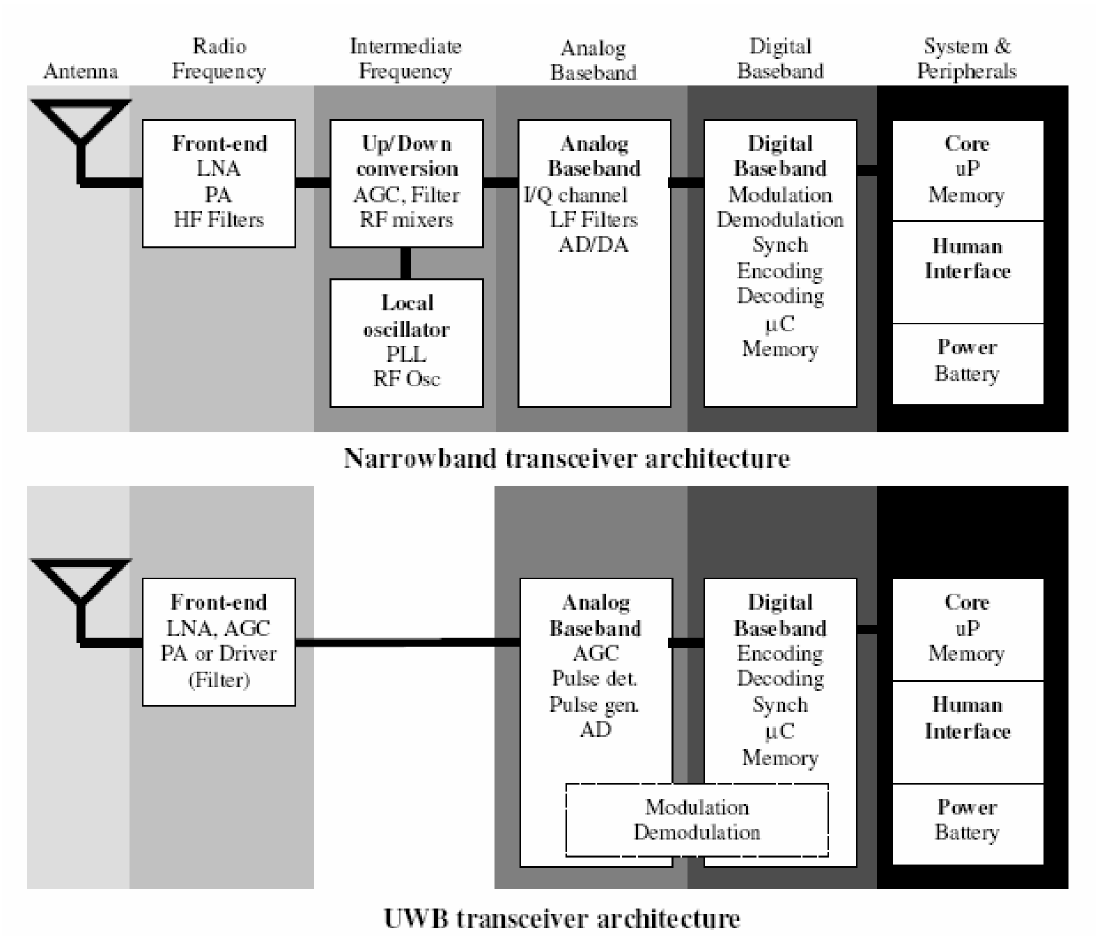

Figure 2.19 : Comparison of UWB and narrowband transreceivers.

Table 2.4: Comparison Summary [11]

	Ultra-Wideband	**Narrowband**
Antennas	Small antenna design with gain and wideband matching with few components is difficult. Antenna and front-end co-design is necessary.	Small high Q antenna design with good gain is easily achievable 50Ω impedance easy to match. Antenna and front-end can be designed independently.
RF front-end	Wideband LNAs are power consuming and hard to match. Relaxed requirement of linearity. Partial filtering achieved by antenna.	Narrowband LNA are easy to match. Non constant envelope modulation (e.g. OFDM) need very high linearity Tough filtering is needed to satisfy out-of-band emission.
Intermediate frequency	No need.	AGC, Mixers, RF oscillator, PLL
Analog baseband	Very high bandwidth A/D converters Extended time sampling techniques Digital sampling oscilloscope techniques	Small bandwidth A/D converter (typically twice the data rate)
Digital baseband	Coherent detection of very fine time resolution Precise time references	Non-coherent detection
Other aspects	On-board noise External jammer Channel characteristics is not completely known studies still on going	Load-pull LO leakage LO pulling by PA Narrow channels are well defined.

3. SILICON-GERMANIUM HETEROJUNCTION TRANSISTORS

The heterojunction bipolar transistor (HBT) is an improvement of the bipolar junction transistor (BJT). It contains different semiconductor materials than BJT in emitter and base regions to create a heterojunction. Arsenide, indium, gallium, phosphide and germanium are possible materials which have been used to improve the performance of BJT.

In this chapter a general view is preserved for Silicon-Germanium (Si-Ge) heterojunction bipolar transistors. Since the LNA circuit in the next chapter is designed by using SiGe BiCMOS process, a brief description which contains a comparison with CMOS technology and the last improvements is given in the subtitles.

3.1 Bandgap Engineering in Silicon

The word bandgap or energy gap is the difference between the top of the valence band and the bottom of the conduction band, which is found in insulators, and semiconductors. A semiconductor can be defined as a material, which has a bandgap between 0 and 3eV. Semiconductors can be defined as a kind of insulators with a narrow band gap. Electrons are able to jump from one band to another. An electron to jump from a valence band to a conduction band but it needs a specific minimum amount of energy for the transition. This required energy is a specific property for materials and can be provided by absorbing either a phonon (heat) or a photon (light) [12].

Silicon, which is the vital semiconductor for microelectronics, is one of the three most plentiful elements in Earth. It has some practical advantages that lead Si to be widely used and to dominate the semiconductor market.

Si is not only very abundant; it can also be purified without much effort. Si crystals can be grown in amazingly large, virtually defect-free single crystals. The resultant large Si wafer size translates directly into more integrated circuits per wafer, lowering the cost per IC. Given that a 200 mm Si boule is roughly 6 feet long, Si crystals are literally the largest and perfect on the face of planet Earth. Its thermal conductivity is large (77 K) and it removes the dissipated heat efficiently. Different material forms that contain Si are very useful for integrated circuit technologies. These forms are crystalline Si, polycrystalline Si (poly Si), and amorphous Si. Also, it can be etched easier than its competitors. The diamond lattice cyrtsal structure of Si is main reason of its excellent mechanical properties which make the fabrication process easier. The magnitude of energy bandgap of Si is acceptaple (1.12eV at 300K). If the bandgap were smaller than 0.5eV, the intrinsic carrier density would be too large at 300 K, making parasitic off-state leakage currents too large. If the bandgap were larger than 2eV, then typically it becomes difficult to etch and diffuse dopant impurities [13-14].

These properties make the Si wonderful from the IC fabrication point. However, Si is not the ideal semiconductor from the perspective of integrated circuit designers. The carrier mobility for electrons and holes of Si is smaller than III-V elements. The maximum achievable velocity is $1x10^7$cm/sec for the carriers in Si under very high electric fields. The speed of a transistor is determined by how fast the carriers can be transported thought the device under meaningful operating voltages. Under this fact, Si is an insufficient semiconductor [15].

The steady-state velocity of the charge is known as its drift velocity ν_d. The drift velocity is depended to the electric field. At fields below a specific level, the carriers obey Ohm's law. The drift velocity increases linearly with the electric field as seen in (3.1) where μ is mobility and E is applied electric field. At higher fields, the carrier velocity becomes a sublinear function of the electric field and saturates at a velocity. This leveling-off of the carrier drift velocity at high field is known as velocity saturation [13].

$$\nu_d = \mu.E \tag{3.1}$$

Mobility is a measure of the time interval between collisions for a carrier moving through a semiconductor lattice. The two most important collision mechanisms in bipolar transistors are lattice and impurity scattering, and the total mobility is given by the sum of the probabilities of collisions due to these individual mechanisms [13]:

$$\frac{1}{\mu} = \frac{1}{\mu_I} + \frac{1}{\mu_L} \tag{3.2}$$

Lattice scattering is caused by collisions between carriers and the atoms of the semiconductor lattice. It is the thermal vibration causes the displacement of these lattice atoms from their lattice sites. It disrupts the perfect periodicity of semiconductor lattice. Since temperature increases thermal motion μ_L decreases with temperature [14].

Impurity scattering is caused by collisions between carriers and impurity atoms in the semiconductor lattice. Impurity or dopant atoms have the effect of disrupting the perfect periodicity of the semiconductor lattice, and the amount of disruption increases with impurity concentration. The mobility due to impurity scattering μ_I therefore decreases with increasing impurity concentration [15].

Moreover, since Si is an indirect gap semiconductor, light emission is inefficient, which makes the implementation of active optical devices such as diode lasers impractical. The electronic properties of a semiconductor are dominated by the highest partially empty band and the lowest partially filled band, it is often sufficient to only consider those bands. In Figure 3.1 there is a simplified energy band diagram for semiconductors.

In Figure 3.1, line E_c is the bottom edge of the conduction band, and the top of the valence band is indicated by the line E_v. The energy band gap, E_g, is located between these bands. The distance between the conduction band edge, E_c, and the energy of a free electron outside the crystal (called the vacuum level; E_{vacuum}) is quantified by the electron affinity, c multiplied with the electronic charge q.

The minimum of the conduction band and the maximum of valence band can occur at the same value for the wavenumber. If so, the energy bandgap is called direct bandgap. Otherwise, the energy bandgap is called indirect bandgap. This distinction is of interest for optoelectronic devices since direct bandgap materials provide more efficient absorption and emission of light [16].

Many of compound semiconductors of groups III and V such as gallium arsenide (GaAs), indium phosphide (InP), aluminium gallium indium phosphide (AlGaInP) have higher mobilities, and saturation velocities. Unlike Si, they are also able to make efficient optical generation and detection devices because of their direct energy gap characteristic. III–V devices, by virtue of the way they are grown, can be compositionally altered for a specific need or application. This atomic-level custom tailoring of a semiconductor is called bandgap engineering, and results a large performance advantage for III–V technologies over Si [13].

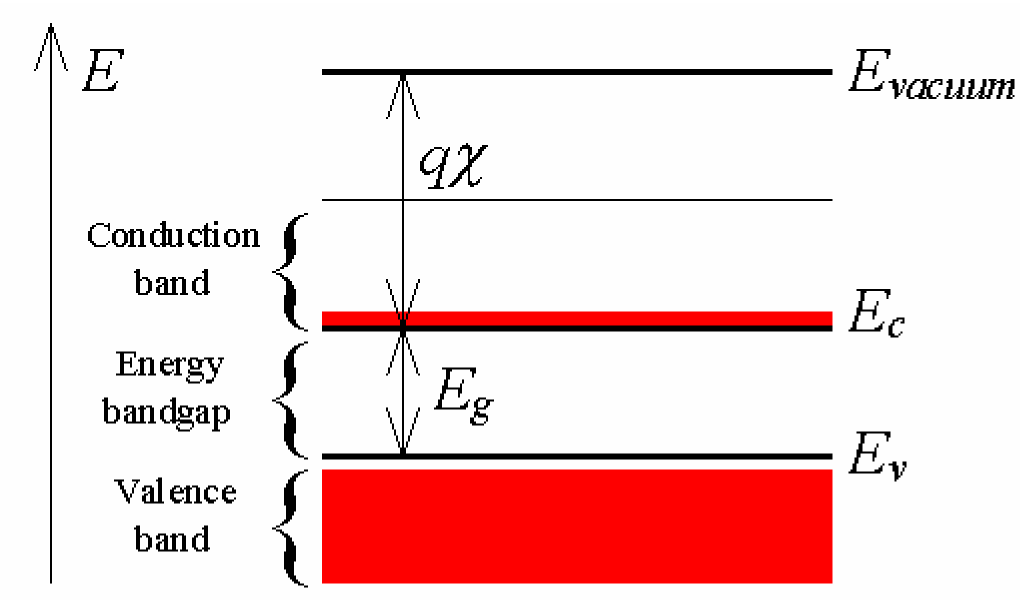

Figure 3.1 : A simplified energy band diagram for semiconductors.

Bandgap engineering is an impressive and strong technique for desinging new semiconductor materials and devices. Heterojunctions and modern growth techniques, such as molecular beam epitaxy, allow band diagrams with nearly arbitrary and continuous band-gap variations to be made. The transport properties of electrons and holes and thus the capabilities of materials can be independently and sustainably tuned for a given application [12-16].

Even though III–V semiconductors have large number of benefits in performance outcomes, they own also insuperable disadvantages in making low cost integrated circuits. There is no durable thermally grown oxide for GaAs or InP, for instance, and wafers are smaller with much higher defect densities, are more prone to breakage, and are poorer heat conductors. These imperfections cause lower levels of integration, more difficult fabrication, lower yield, and ultimately higher cost.

Today, groups III–V materials such as GaAs and InP fill are important for proper applications in specific markets (e.g. lasers based on AlGaAs- or InP) but III–V from the point of the ones in semiconductor technologies they will never become dominant in the infrastructure of the communications revolution if Si-based technologies fulfill the requirements of jobs [14].

Researches in material science and compound semiconductor electronics focus on the idea of improving the performance of Si transistors enough to be competitive with III–V devices for high-performance applications, while preserving the enormous yield, cost, and manufacturing advantages associated with conventional Si fabrication, because even Si integrated circuits are suitable for high-transistor count, high volume microprocessors and memory parts, they cannot provide enough performance and satisfy the demands in higher frequency operations such as circuits for RF, microwave, and millimeter-wave (mm-wave) electronic applications. Limited high frequency performance of Si devices is caused by poorer intrinsic speed of Si and this suppresses the advantage of being inexpensive. Producing a cheap device which under performs and cannot achieve the given spects in a given frequencies is not acceptable and far from being competative. The expensive but faster III-V technologies will become mainstream for the RF and microwave circuit design (e.g. cell phone power amplifiers).

Improving the high frequency performance of Si while keeping cost and the manufacturing advantages associated with conventional Si fabrication is the key point to overcome to III-V technologies and the products based on these technologies. Combination of Silicon and Germanium is the corresponding technology for this demand. Using SiGe and Si-strained layer epitaxy to practice bandgap engineering in the Si material system conclude as SiGe heterojunction bipolar transistors. This is gift of bandgap narrowing and can be employed in high performance applications to achieve the expectations [16].

Bandgap narrowing uses the fact that the doping reduces the bandgap. Figure 3.2 illustrates the effect of doping on bandgap level of Si:

The energy levels of the dopant atoms are discrete in lightly doped semiconductors, because the dopant atoms are sufficiently widely spaced in the semiconductor lattice Furthermore, it is reasonable to assume that the widely spaced dopant atoms have no effect on the perfect periodicity of the semiconductor lattice, and hence the edges of the conduction and valence bands are sharply defined. Figure 3.2(a) illustrates the energy versus density of states diagram.

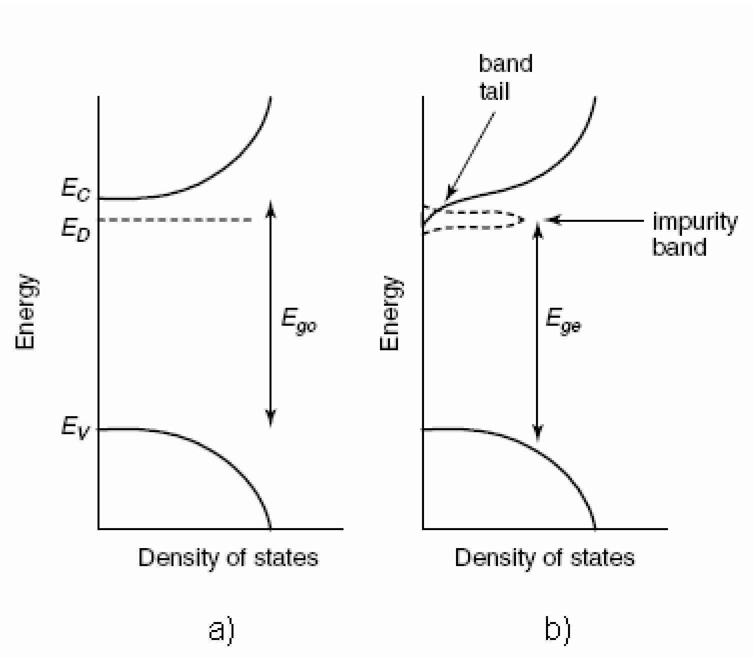

Figure 3.2 : The effect of doping in n-type of Si. a) lightly doped silicon b) heavily doped silicon [13].

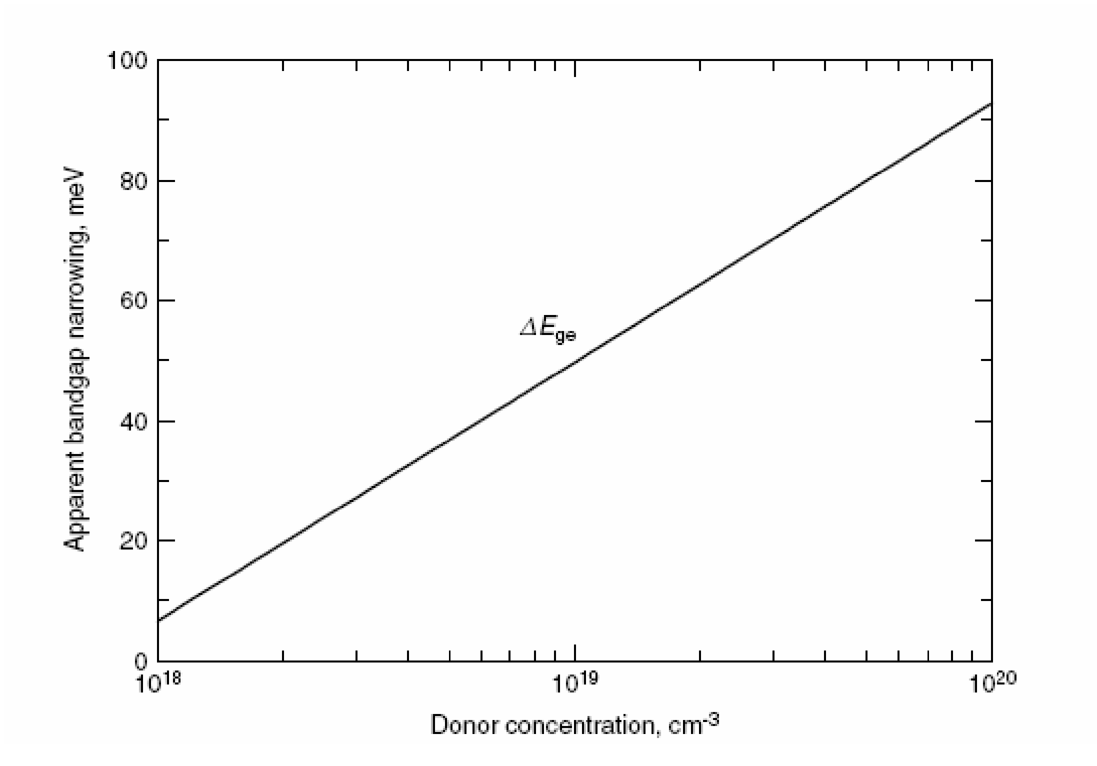

Figure 3.3 : Apparent bandgap narrowing, or induced bandgap narrowing, as a function of donor concentration in n-type Si [13].

On the other hand, the dopant atoms are close enough together in heavily doped semiconductors. This causes the discrete impurity level in Figure 3.2(a) to split and form an impurity band, as shown in Figure 3.2(b). In addition, the large concentration of dopant atoms disrupts the perfect periodicity of the silicon lattice, giving rise to a band tail instead of a sharply defined band edge. The situation is illustrated in Figure 3.5(b) as the energy versus density of states diagram for the case of a heavily doped, n-type semiconductor. It can be seen that the overall effect of the high dopant concentration is to reduce the bandgap from from E_{g0} to E_{ge}. In p-type silicon the situation is same [13].

In general, bandgap narrowing can occur in a heavily doped base, or indeed in the emitter of a pnp transistor.

3.2 SiGe HBT Technology

There are numerous trade-offs between a number of competing mechanisms in the design of bipolar transistors requires. The basewidth (W_B) needs to be very small, in order to achieve fast base transit time (τ_B), and hence a high value of cut-off frequency. This relationship is shown in equation (3.3) where D_{nb} is diffusion coefficient of electrons in the base [13]:

$$\tau_B = \frac{W_B^{\,2}}{2D_{nb}} \tag{3.3}$$

Hence, it is the limiting factor; basewidth can be reduced by punch-through of the base. It occurs with the intersection of emitter/base depletion region to the collector/base depletion region in the base. Figure 3.4 pictures the punch-through.

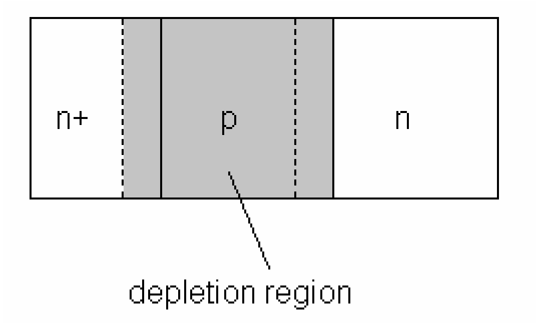

Figure 3.4 : Bipolar transistors operating in punch-through.

Punch-through is not a choice but it is a limit for silicon bipolar transistors since its electrical effect –flowing huge current between emitter and collector- is same with junction breakdown. State-of-art, silicon bipolar transistors typically have basewidths of much less than 0.1μm, and therefore often operate close to the punch-through limit which requires spectacular transistor and process design [13].

The increase in the base doping concentration results thinner depletions region and thus narrower basewidths. This introduces an opportunity to improve the performance of silicon bipolar transistors. However, there is an inverse proportion between current gain (β) and the base doping. The ratio of base and emitter doping concentrations strongly affects the gain. The relation in (3.4) shows that to obtain high gain the emitter doping concentration (N_{de}) should be high and the base doping concentration (N_{ab}) should be low [13].

$$\beta = \frac{D_{nb} \cdot W_E \cdot N_{de}}{D_{pe} \cdot W_B \cdot N_{ab}} \qquad \textbf{(3.4)}$$

This trade-off between gain and base transit time is the essential limiting factor of maximum achievable cut-off frequency of a silicon bipolar transistor. Implementing cut-off frequencies much higher than 50GHz in silicon bipolar transistors is technologically difficult [13-14].

Table 3.1 gives the basic properties of Silicon and Germanium [17]. As a result of the issues that have been explained so far, Si which haves larger bandgap and Ge which haves higher bandgap can be combined to achieve an alloy (SiGe) that owns an energy bandgap lower than Si. A bipolar transistor could be created with placing this alloy in the base region and Si in the emitter region and its gain would be much higher than traditional bipolar transistor while having reduced basewidths and increased base doping [12-16, 18-19]. The usage of this bandgap engineering method brings silicon germanium heterojunction bipolar transistors with higher valued cut-off frequencies as compared with Si bipolar junction transistors. Cut-off frequency can be reach up to 350GHz in SiGe HBT technology [20].

As seen in Figure 3.5 a SiGe HBT is produced by placing the SiGe base between Si collector and Si emitter. The bandgap difference of SiGe and Si mainly occurs in the valence band. Therefore the bandgap difference in the valance band is seen as discontinuities at the emitter/base and collector/base heterojunctions, while it is seen as spikes in the conduction band. The illustration in Figure 3.6 shows the energy band diagrams of SiGe HBT in a comparative way with Si BJT where the dashed line is for SiGe HBT and the solid one is for Si BJT. Normally the spike in conduction band is very small which makes its effect meager on the transistor's electrical behaviours.

Table 3.1: Basic properties of Silicon and Germanium [17]

Basic Properties	**Si**	**Ge**
Crystal structure	diamond	diamond
Lattice constant [nm]:	0.5431	0.565
Density [g/cm^3]	2.329	5.32
Atomic concentration [cm^{-3}]	$5x10^{22}$	$4.4x10^{22}$
Melting point [^oC]	1414	937
Thermal conductivity [W/cm ^oC]	1.3	0.58
Thermal expansion coefficient [1/^oC]	$2.6x10^{-6}$	$5.9x10^{-6}$
Dielectric constant	11.7	16.2
Index of refraction	3.42	4.00
Energy gap [eV]	1.12	0.66
Type of energy gap	indirect	indirect
Drift mobility Electron [cm^2/V sec]	≤ 1400	≤ 3900
Drift mobility Holes [cm^2/V sec]	≤ 450	≤ 1900
Breakdown field [V/cm]	$\approx 3 \cdot 10^5$	$\approx 10^5$
Diffusion coefficient electrons [cm^2/s]	≤ 36	≤ 100
Diffusion coefficient holes [cm^2/s]	≤ 12	≤ 50
Electron thermal velocity [m/s]	$2.3 \cdot 10^5$	$3.1 \cdot 10^5$
Hole thermal velocity [m/s]	$1.65 \cdot 10^5$	$1.9 \cdot 10^5$

Another result that can be obtained from Figure 3.6 is smaller conduction band barrier level (E_b) in SiGe HBT. Its meaning is collector current at a specific base/emitter voltage will be bigger in a SiGe HBT than in a Si BJT. On the other hand, it can be implied that the base currents of the two types of device will be approximately the same since barrier height of the valence band is almost the same in the SiGe HBT and the Si. That is the reason of increased gain in SiGe technology [13-15].

From different point of view, for the same value of collector current, SiGe HBT dissipates lower power than Si BJT since it needs less V_{BE}.

Figure 3.7 models the mobilities of electrons and holes in $Si_{1-x}Ge_x$ alloys as a function of dopant concentration. The available theoretical models work best for electrons in unstrained n-type bulk material at temperatures above 100 K and doping concentrations below 10^{17} cm^3 [19,20].

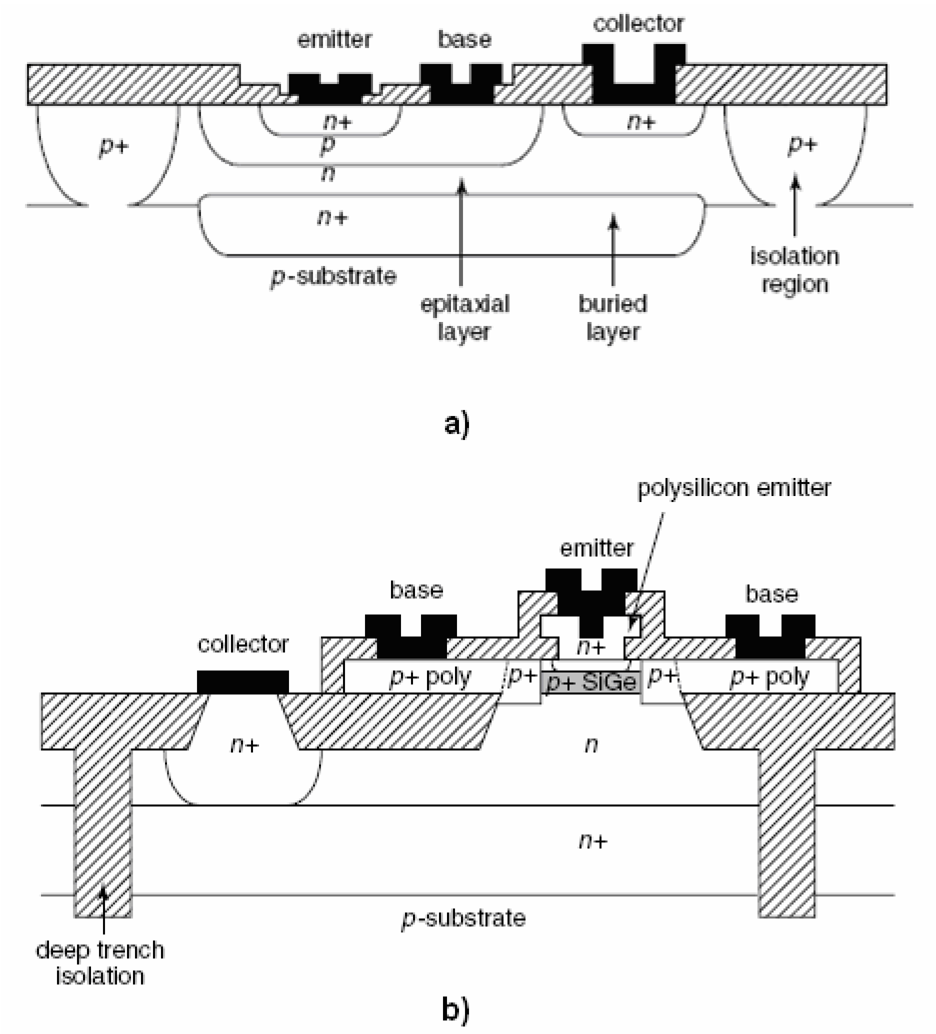

Figure 3.5 : a) Cross section of a basic BJT. b) Cross section of a SiGE HBT.

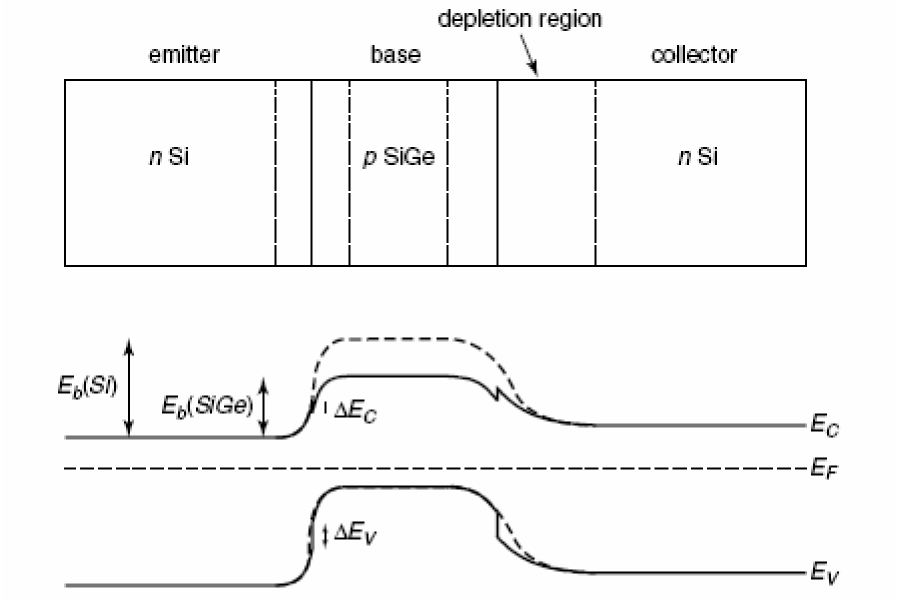

Figure 3.6 : Band diagrams of SiGe HBT and Si BJT.

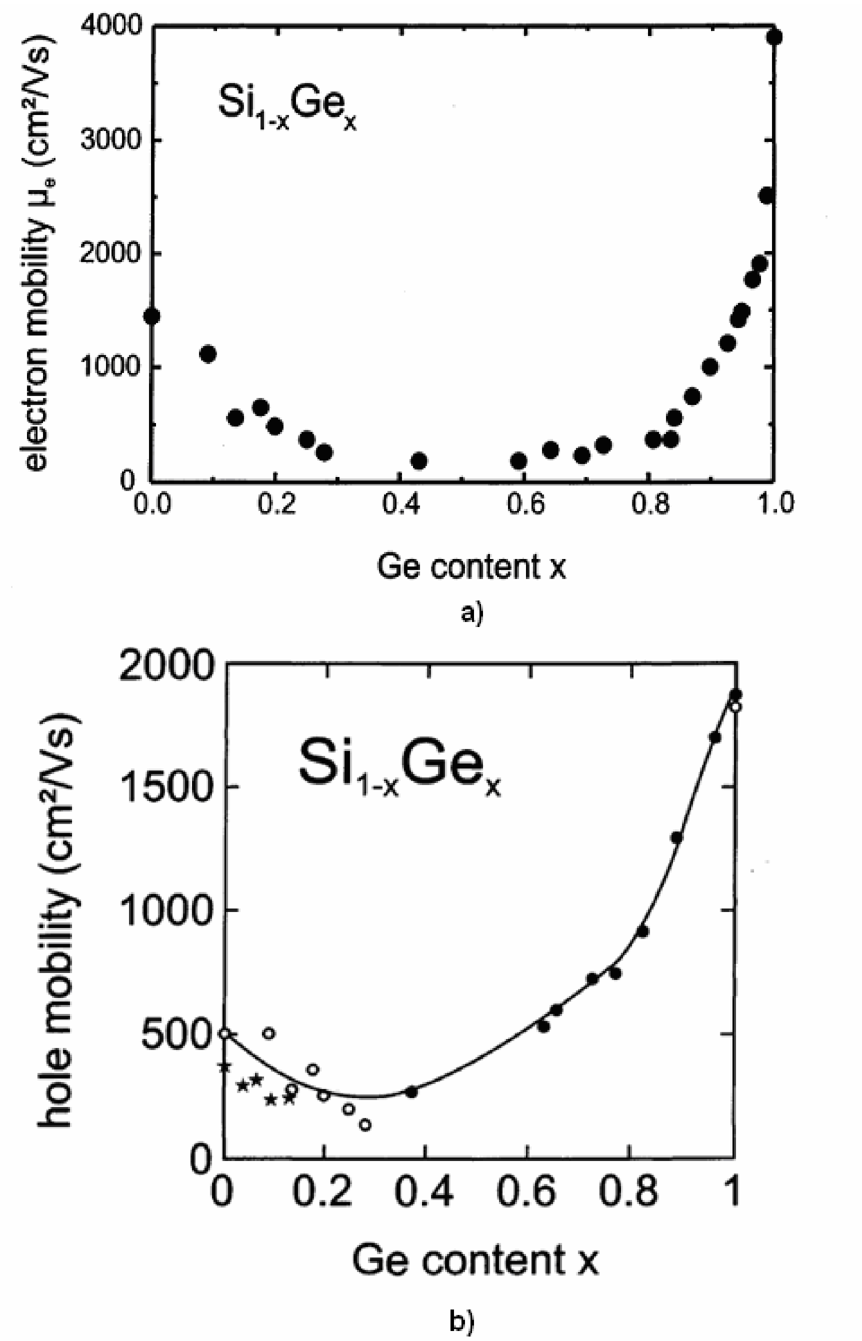

Figure 3.7 : a) Electron mobility versus composition at 300K b) Hole mobility versus composition at 300K [21-22].

3.3 Evolution Path of SiGe HBT Technology

It is an old idea to combine Silicon (Si) and Germanium for transistor engineering. The first transistor patents of Shockley contain the principle of using Germanium in building transistor, which is dating 1951. The first theory and operational concepts were given by Kroemer in 1957. From 30 years then Si-Ge HBT waited to be realized because of the limitations of material science and process technology. After the achievement of necessary technological innovations, the first SiGe HBT was demonstrated in 1987. In the last decade of 1992, the first SiGe bipolar complementary metal oxide semiconductor (BiCMOS) technology was announced. In December 1994, SiGe HBT was started to being used in commercial production [13-14].

Table 3.2: Key steps in SiGe HBT Technology [14]

Historical Event	**Year**
Fundamental HBT patent	1951
Drift-based HBT concept	1954
Basic HBT theory	1957
First growth of SiGe strained layers	1975
First growth of SiGe epitaxy by MBE	1985
First growth of SiGe epitaxy by UHV/CVD	1986
First SiGe HBT	1987
First ideal SiGe HBT grown by CVD	1989
First high performance SiGe HBT	1990
First self-aligned SiGe HBT	1990
First SiGe HBT ECL ring oscillator	1990
First pnp SiGe HBT	1990
First SiGe BiCMOS Technology	1992
First LSI SiGe HBT Integrated Circuit	1993
First SiGe HBT with peak f_T above 100GHz	1993
First SiGe HBT technology in 200mm manufacturing	1994
First SiGe HBT technology optimized for 77K	1994
First SiGeC HBT	1996
First high power SiGe HBTs	1996
First sub-10 psec SiGe HBT ECL circuits	1997
First SiGe HBT with peak f_T above 200GHz	2001
First complementary (npn&pnp) SiGe HBT technology	2003
First SiGe HBT with both f_T and f_{max} above 300 GHz	2004

The 200-GHz peak f_T barrier was passed in late 2001 for a non-self-aligned device [23], and for a self-aligned device in February of 2002 [24].

SiGe HBT technologies with f_T above 300 GHz are clearly a realistic today making SiGe HBTs quite competitive in performance with competing III-V HBT technologies. Today important commercial circuit implementations are using this technology. A 69 x 69 cross-point switch in [25] is an integrated circuit which has a vast number of SiGe HBT. It contains 100,000 of 0.5-μm SiGe HBTs. One of the highest integration levels with SiGe HBT BiCMOS is a single-chip OC-192 10 Gb/s SONET/SDH mapper which has serializer/deserializer, clock and data recovery circuits, and synthesis unit. It contains 6,000 0.5-μm SiGe HBTs and 1,200,000 CMOS transistors [26]. Also, 24GHz transreceiver chip is one of the latest works that was implemented in SiGe BiCMOS technology [27]. Table 3.2 gives the historical background in more details [13-14].

In 1996 First SiGe:C HBT was announced. Adding small amounts of Carbon into the Si/SiGe material system adjusts the strain. C decreased the intrinsic lattice constant [28]. This technology is not the subject of this work.

3.4 SiGe versus Other Technologies

Currently SiGe technology is divided into 4 generations based on having peak f_T values. If it is in the range of 50 GHz as SiGe HBT categorized as "first generation". If its peak f_T is in the range of 100 GHz it correponds to a "second generation" device. In order to be clasified as "third generation" the f_T has to be in the range of 200 GHz. The last category ''fourth generation" devices which requires a f_T value in the range of 300 GHz. Figure 3.8 illustrates this performance evolution [14].

The popular issue is if SiGe technology will position and dominate the existing and future IC market sectors in every kind of application. Theere is growing interest to the SiGe all around the world and there are more than 25 SiGe fabrication units.

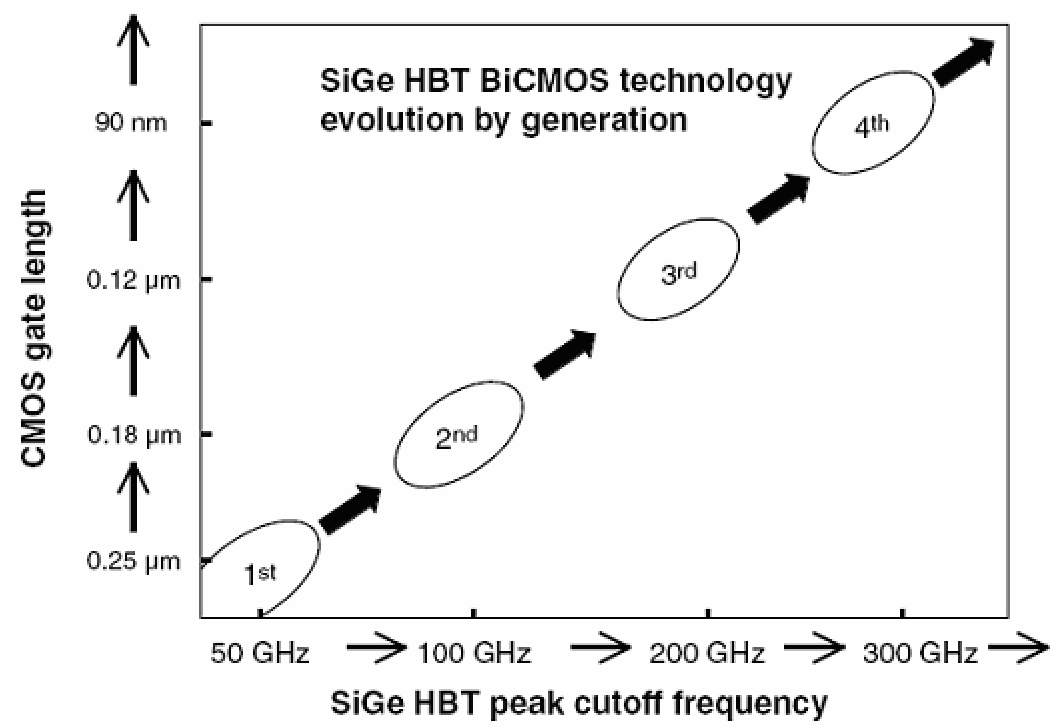

Figure 3.8 : SiGe Technology in terms of CMOS gate length and cut off frequency.

The frequency response, noise figure, and linearity of the new generation SiGe HBTs are comparable to today's III-V devices. Also they are better than both Si BJTs and Si CMOS (even highly scaled CMOS) for these metrics. SiGe HBTs offer better low-frequency (1/f) and phase noise than all of the competition, with the possible exception of Si BJTs [29]. These properties provides advantages in RF design. Hence it is bipolar transistor, the transconductance per unit area of a SiGe HBT is much higher than for either Si or III-V FETs. Also Si or III-V FETs cannot reach the output conductance values of graded Ge based SiGe HBTs. Another benefit of using SiGe HBTs instead of FETs (Si or III-V), is providing the minumum broadband noise level at very low current densities (typically 10 times lower than peak f_T) which makes them very attractive from a power dissipation point of view for portable applications.

Table 3.3: Performance compression of various fabrication technologies

Performance Metric	SiGe HBT	Si BJT	Si CMOS	III-V MESFET	III-V HBT	III-V HEMT
Frequency response	Very good	Good	Good	Very good	Excellent	Excellent
1/f and phase noise	Excellent	Very good	Fair	Poor	Good	Poor
Broadband noise	Very good	Good	Good	Very good	Very good	Excellent
Linearity	Very good	Very good	Very good	Excellent	Very good	Excellent
Output conductance	Excellent	Very good	Fair	Fair	Excellent	Fair
Transconductance /area	Excellent	Good	Poor	Fair	Excellent	Fair
Power dissipation	Excellent	Excellent	Fair	Fair	Very good	Good
CMOS integration	Excellent	Excellent	N/A	Poor	Poor	Poor
IC cost	Good	Good	Very good	Fair	Fair	Poor

III-V devices, especially high-electron-mobility transistors (HEMTs), will continue to provide the very best noise performance, albeit at a higher cost, and given their larger bandgaps and hence breakdown voltages, III-V devices will make the best power devices. System-level integration and cost are two spects that SiGe will continue as winner of the competition for long years because of easy integration of SiGe HBTs and CMOS. This is what III-V technologies cannot do. SiGe is in the same category with Si technology and it is rising on the advantages of Si IC manufacturing, including yield and die cost. Table 3.3 simplifies the overall comparisions between SiGe HBT, Si BJT, Si CMOS, III-V MESFET, III-V HBT and III-V HEMT. The properties; frequency response, noise, linearity, output conductance, transconductance/area, power dissipiation, interagration and costs are compared labeled as five different level [13, 14, 29-31].

3.5 Operating Properties of SiGe HBT

In this part some static and dynamic characteristics are given for SiGe HBT transistors.

3.5.1 Bipolar junction transistors overview

The operation of bipolar transistor is depented to the external bias which must be applied to the emitter/base and collector/base junctions in order to use the device for eletronics applicaltions. These two junctions provide four possible bias configurations, as illustrated in Figure 3.9. The forward active mode of operation is the most useful, because in this configuration the gain of the transistor can be exploited to produce current amplification. A forward bias of approximately 0.6V is applled to the base emitter junction and a reserve bias to the collector/base junction.

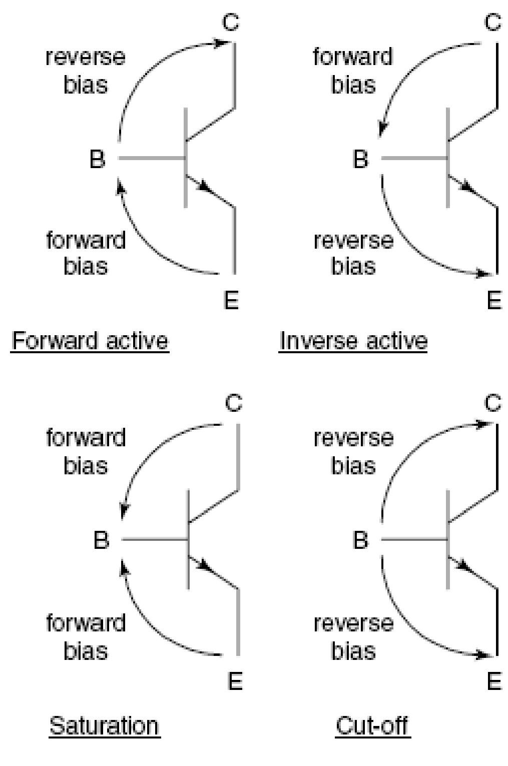

Figure 3.9 : Four operating regions of BJT.

The band diagram for the bipolar transistor operates in forward active region is shown in Figure 3.10. Fermi levels in the emitter, base and collector is seperated by the applied bias voltage. This seperation is being equal to the applied bias. The forward bias across the emitter/base junction leads to a decrease in the potential barrier between the emitter and base, whereas the reverse bias across the collector/base junction leads to an increase in the potential barrier between the base and collector [13].

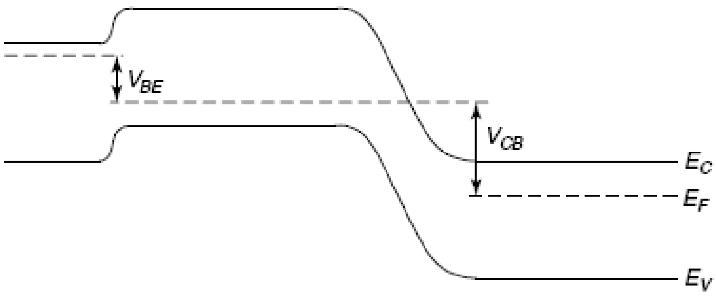

Figure 3.10 : Bipolar transistor biased in forward active region.

In the inverse active mode and saturation modes the transistor can be viewed as open and closed switches respectively which means it is not useful The electrical properties of a bipolar transistor can be characterized by a number of electrical parameters, the most important of which is the common emitter current gain β. This is the ratio of collector current to base current:

$$\beta = \frac{I_C}{I_B} \quad \textbf{(3.5)}$$

In the forward active mode, large number of electrons are injected from the emitter into the base because of the forward biasing of the emitter/base junction. A concentration gradient is therefore established in the base, which encourages the electrons to diffuse towards the collector. If the base of the transistor were very wide all the injected electrons would recombine before reaching the collector, and the transistor would merely behave like two back-to-back diodes. However, the essence of the bipolar transistor is that the base is sufficiently narrow that the majority of electrons reach the collector/base junction, where they are swept across into the collector by the large electric field across the reverse biased junction. This is achieved by making the basewidth comparable with, or smaller than, the diffusion length of electrons in the base. The number of holes which are injected from the base into the emitter determines the base current. Doping the emitter much more heavily than the base makes the base current much smaller than the emitter current. A related electrical parameter to the common emitter current gain is the common base current gain α, which is the ratio of the collector current to the emitter current:

$$\alpha = \frac{I_C}{I_E} \quad \textbf{(3.6)}$$

It is obivous that the sum of collector and base currents gives the emitter current and there is a relation between current gains:

$$I_E = I_B + I_C \quad \textbf{(3.7)}$$

Then,

$$\alpha = \frac{\beta}{1+\beta} \quad \textbf{(3.8)}$$

The common emitter and common base current gains can be measured by biasing the transistor into the forward active region and taking readings of base, emitter and collector current. Three alternative circuit configurations are possible, depending upon which terminal is common between the input and output. These are named as common emitter, common base and common collector circuit configurations. These configurations are going to be used to design amplifier in the next chapter.

The common emitter current gain β is obtained by connecting the transistor in the common emitter configuration, as shown in Figure 3.11(a). The common emitter current gain is obtained by reading off the value of collector current obtained for one of the values of base current and taking the ratio. The common base current gain α can be measured by connecting the transistor in the common base configuration showed as in Figure 3.11(b), and plotting the collector current as a function of collector/base voltage, with the emitter current as a parameter. The common base current gain is obtained by reading off the value of collector current obtained for one of the values of emitter current and taking the ratio [13].

These gain expressions has to be modified because of the heavy doping effects and these modifications in (3.9) and (3.10) lead us to the equation in (3.4):

$$I_B = \frac{qAD_{pe}n_{io}^2}{W_E N_{deff}} \exp\frac{qV_{BE}}{kT} \quad \textbf{(3.9)}$$

$$I_C = \frac{qAD_{nb}n_{io}^2}{W_B N_{deff}} \exp\frac{qV_{BE}}{kT} \quad \textbf{(3.10)}$$

In equations above D_{nb} is diffusion coefficient of the electrons in the base and D_{pe} is the diffusion coefficient of the holes in the emitter. N_{deff} is the effective doping concentration which includes the effects that come from band narrowing. A is the area of the emitter-base junction. It is imported to notice that the intrinsic carrier concentration of lightly doped Si (n_{io}) is also effective in equations (3.9) and (3.10).

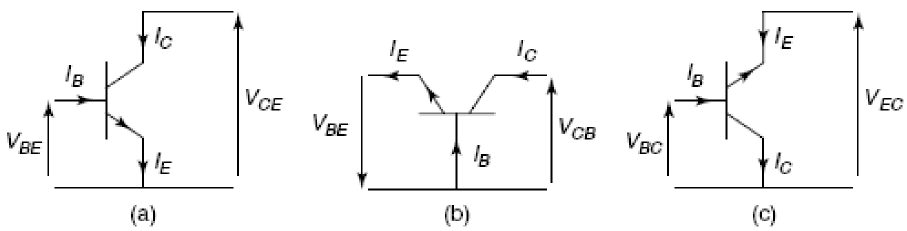

Figure 3.11 : Possible configurations of a bipolar transistor a) CE b) CB c) CC.

The most important high frequency parameter of bipolar transistor is cut-off frequency f_T which can be defined as the frequency that the gain drops to unity. It is seen on Figure 3.12. The cut-off frequency can be derived by using small signal hybrid π model of the transistor.

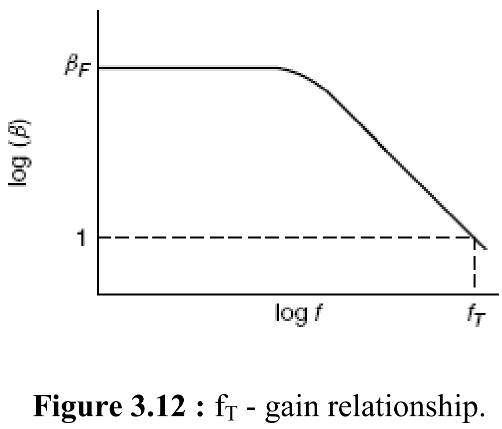

Figure 3.12 : f_T - gain relationship.

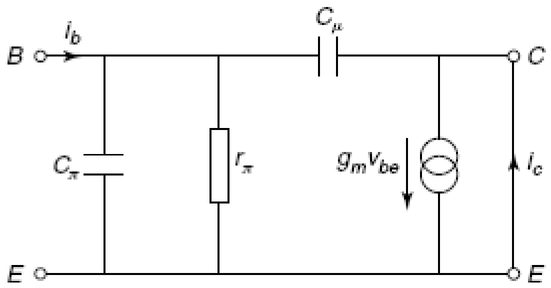

Figure 3.13 : Small signal π model of the transistor [13].

For the circuit given in Figure 3.13 the following equations can be written:

$$i_c = g_m v_{be} - j\omega C_\mu v_{be} \qquad \textbf{(3.11)}$$

$$i_b = v_{be}\left(g_\pi + j\omega C_\pi + j\omega C_\mu\right) \qquad \textbf{(3.12)}$$

where $g_\pi = 1/r_\pi$ and $\omega = 2\pi f$. C_μ is the collector/base depletion capacitance and C_π is the sum of the emitter/base depletion capacitance and the emitter diffusion capacitance. The common emitter current gain can be defined as:

$$\beta = \frac{g_m - j\omega C_\mu}{g_\pi + j\omega C_\pi + j\omega C_\mu} \qquad \textbf{(3.13)}$$

For the frequencies in the interested band, $g_m >> j\omega C_\mu$ which leads 3.14:

$$\beta = \frac{\beta_F}{1 + j\omega r_\pi\left(C_\pi + C_\mu\right)} \qquad \textbf{(3.14)}$$

Since β_F is the common emitter current gain at low frequencies:

$$\beta_F = g_m r_\pi \qquad \textbf{(3.15)}$$

At high frequencies the denominator of (3.14) can be simplified:

$$|\beta| = \frac{\beta_F}{\omega r_\pi\left(C_\pi + C_\mu\right)} \qquad \textbf{(3.16)}$$

The gain becomes 1 when:

$$1 = \frac{\beta_F}{2\pi f r_\pi \left(C_\pi + C_\mu\right)} \quad \textbf{(3.17)}$$

Also the model based termination in (3.18) can be used to achieve (3.20):

$$r_\pi = \frac{kT}{qI_B} \quad \textbf{(3.18)}$$

Since the forward transit time is expressed with using various delay times as follows:

$$\tau_F = \tau_E + \tau_{EBD} + \tau_B + \tau_{CBD} \quad \textbf{(3.19)}$$

$$f_T = \frac{1}{2\pi\left(\tau_F + \frac{kT}{qI_C}\left(C_{JE} + C_{JC}\right)\right)} \quad \textbf{(3.20)}$$

C_{JE} and C_{JC} are the emitter/base and base/collector depletion capacitances. The results shows that f_T increases with collector current. However, as Figure 3.14 illustrates that at higher current effects start after a current level and.

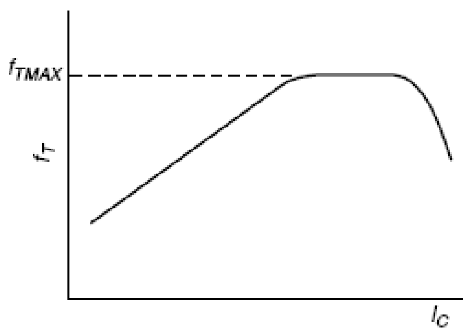

Figure 3.14 : f_T versus collector current characteristics [13].

3.5.2 SiGe hetero junction bipolar transistors characteristics

3.5.2.1 Current-gain properties of SiGe HBT

Since the conduction band spike in a SiGe HBT is very small, the same approach with (3.10) and (3.11) can be used to calculate the collector current of a SiGe HBT. The following equation can be derived for SiGe HBT:

$$I_C = \frac{qA(D_{nb})_{SiGe}(n_i^2)_{SiGe}}{W_B N_{deff}} \exp\frac{qV_{BE}}{kT} \quad \textbf{(3.21)}$$

N_{deff} is same in SiGe andb Si. The intrinsic carrier concentration for SiGe can be given as:

$$\left(n_i^2\right)_{SiGe} = n_{io}^2 \exp\frac{\Delta E_G}{kT}\left[\frac{(N_C N_V)_{SiGe}}{(N_C N_V)_{Si}}\right] \quad \textbf{(3.22)}$$

Using (3.22) inside (3.21) and taking the ratio of the collector currents give us the enhancement in the current gain of SiGe HBT.

$$\frac{\beta_{SiGe}}{\beta_{Si}} = \frac{\left(N_C N_V D_{nb}\right)_{SiGe}}{\left(N_C N_V D_{nb}\right)_{Si}} \exp\frac{\Delta E_G}{kT} \quad \textbf{(3.23)}$$

N_C and N_V are effective density of states in the conductance and valance bands, respectively.

3.5.2.2 Cut-off frequency of SiGe HBT

A key SiGe HBT AC figure-of-merit, unity gain cutoff frequency (f_T), can be written as follows [13]:

$$f_T = \frac{1}{2\pi\tau_{ec}} = \frac{1}{2\pi}\left[\frac{kT}{qI_C}\left(C_{te} + C_{tc}\right) + \tau_b + \tau_e + \frac{W_{CB}}{2v_{sat}} + r_c C_{tc}\right]^{-1} \quad \textbf{(3.24)}$$

where $\frac{kT}{qI_C} = g_m$, C_{te} and C_{tc} are the EB and CB depletion capacitances, τ_b is the base transit time, τ_e is the emitter charge storage delay time, W_{cb} is the CB space–charge region width, v_{sat} is the saturation velocity, and r_c is the dynamic collector resistance. τ_{ec} is the total emitter-to-collector delay time, and sets the ultimate limit of the switching speed of a bipolar transistor. Therefor, under fixed bias current, having an improvement in τ_b and/or τ_e –because of using SiGe- makes an enhancement in f_T and f_{max} of the transistor at fixed bias current. ''Maximum oscillation frequency'' a figure-of-merit (fmax) can be given as follows:

$$f_{\max} = \sqrt{\frac{f_T}{8\pi C_{bc} r_b}} \quad \textbf{(3.25)}$$

where r_b is the small-signal base resistance, and C_{bc} is the total collector–base capacitance. In order to increase the maximum power gain and circuit operating frequency, f_T should be larger while r_b, and C_{bc} are smaller.

3.5.2.3 Output conductance of SiGe HBT

Another vital parameter for a transistor is dynamic output transconductance which is desired to be zero (equals to infinite output resistance). On the other hand, unlike the ideal case increasing V_{CB}, degrades base region from the backside. It means a movement occurs in moving neutral boundary of base. W_b is a role in the minority carrier density on CB side of the neural base. That's why the collectror current rises. Finite base doping leads to the situation that I_C and V_{CB} increases simulatenously. This clearl gives a finite output conductance. This is a well known issue called "Early effect". The Early voltage is a simple and convenient measure of the change in output conductance with changing V_{CB}. The value of this parameter (V_A) is defined as follows in SiGe HBT [14]:

$$V_{A,SiGe} = \left[\frac{-D_{nb}(W_b)\, n_{ib}^2(W_b)}{p_b(W_b)} \int_0^{W_b} \frac{p_b(x)\, dx}{D_{nb}(x)\, n_{ib}^2(x)} \right] \left[\frac{\partial W_b}{\partial V_{CB}} \right]^{-1} \quad \textbf{(3.26)}$$

V_A depends exponentially on the difference in bandgap between $x = W_b$ and that region in the base where n_{ib} is smallest. That is, the base profile is eöectively "weighted" by the increasing Ge content on the collector side of the neutral base, making it harder to deplete the neutral base for a given applied V_{CB}, all else being equal, effectively increasing the Early voltage of the transistor.

4. UWB LOW NOISE AMPLIFIER DESIGN

SiGe BiCMOS is becoming the technology of choice for achieving cost-effective integration in wireless and wireline communication transceivers. In this chapter, operating principles, noise and gain characteristics of a SiGe HBT are given at first. Then possible low noise amplifier topologies are analyzed. Finally a new topology is proposed.

4.1 UWB LNA Design Overview

Low noise amplifier is the first component of a receiver. Because of this it has got big impact on the noise figure of the over all system. It has to provide sufficient gain while increasing the noise as little as possible. Its gain should deal with the noise of the previous stages successfully. LNA should work with large signals without distortion and must present specific input impedance often 50Ω. This is important because LNAs usually com after passive filters and must satisfy this requirement.

The major titles that must be considered in a LNA design are; gain, noise, power consumption and input impedance. On the other hand the supply voltage is very limited and while the linearity should satisfy a good characteristic [32].

Although these terms on Figure 4.1 are not directly proportional with each there are lots of strategies for LNA design that optimize the noise figure while providing high voltage gain, good input match and low power consumption simultaneously. On the other hand ultra-wideband LNA design has got its own challenges different than narrowband design [32-33].

Broadband input and output impedance matching, frequency response flattening over the whole band of interest spot and mean noise figure constraints and power consumption are the key points in the design. Since frequency band is regulated by stringent power constraints, noise issues have to be carefully taken into account with respect to the narrowband design.

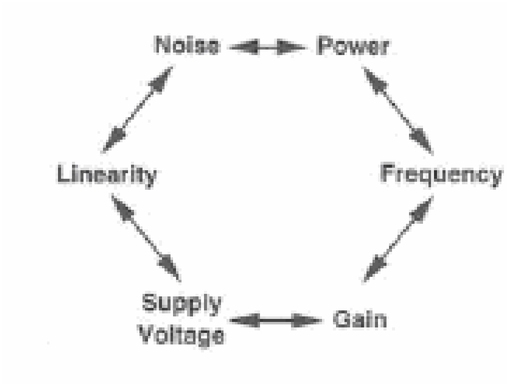

Figure 4.1 : RF design hexagon.

The input and output impedance matching can be best achieved by passive networks such as filters or ladder matching networks. On the other hand, extra noise introduced to the LNA input by the passive elements. Also, the mismatches caused by the inductors reduce the design reliability.

There are several different topologies that use CMOS or SiGe HBTs in previously published papers. The different CMOS topologies are filter configuration [34-35], feedback configuration [36] and distributed amplifiers [37]. SiGe ultrawide band low noise amplifiers also utilize resistive feedback [38], Darlington amplifier [39], cascode amplifier with emitter degeneration [40] and distributed amplifier topologies [41].

Distributed amplifier topology features good broadband operating characteristic by removing the effect of the first transistor's parasitic capacitance with the transmission line. This transmission line can be realized by LC ladder network. However, the large area and high power consumption appear as problems for UWB LNA design.

Unlike distributed amplifiers, it is a big challenge to achieve a good noise figure with a high gain over a wide frequency range with feedback topology in CMOS design. SiGe HBT can satisfy high gain with lower voltage levels but limited input match brings problems in high frequencies.

Darlington transistor pairs provide high gain which is good for UWB usage. It can be supported with feedback configuration to improve the performance but input matching is not enough to satisfy UWB specs. Moreover, high power consumption is another disadvantage [40].

Lowest noise figures can be achieved with emitter degenerated cascode amplifier architectures but their narrow band nature brings vital problems for matching. Placing a filter configuration can enhance performance but it is still difficult to reach high gain levels.

Balanced amplifier topology is another possibility which is used in several papers with HBT or HEMT choices [42-44]. The flatness of the gain characteristic is very good and the matching characteristics are excellent in balanced amplifiers, but these architectures require Lange couplers which are difficult to design and fabricate. These couplers have also negative effects in noise figure. Moreover large die size is another handicap for the design.

There are two widely used choices in CMOS UWB LNA design for the first stage and the following stages; common source [34] and common gate amplifiers [35, 45]. On the other hand common base and common emitter amplifiers are corresponding configurations for SiGe HBT low noise amplifiers [46, 47]. It is very popular to configure low-noise amplifiers as common-emitter or common-source amplifier circuits configuration which is a useful way to minimize the noise figure of the amplifier over a narrow frequency range. However, the performance of common-gate is better than common-source in input matching, reserve isolation and stability [33]. Similarly, common-base configuration with SiGE HBTs outperforms common-emitter configuration [46-48]. The large parasitic capacitance between the base and emitter nodes dominates input impedance of the transistor since it suffers from Miller effect. As a result, input matching over a wide frequency range is difficult to achieve. A reactive matching network can be one solution for broad band matching, but an amplifier based on this approach would draw a relatively large current. Another issue is isolation which means the value of feedback from output to input. The isolation is very strong in common base amplifiers. It was seen that under many situations the CB topology offers significant advantages over the CE configuration for amplifier applications [48]. Also according to the measurements the linearity of common base configuration gives better results than common emitter configuration [49].

4.2 UWB LNA Design Overview

Low-frequency noise, RF noise, and phase noise of SiGe HBTs should be kept at low values in order to achieve high cut-off frequency, low base resistance, and high current gain at the same time. Possible optimization in SiGe profile leads to improvement in f_T and β which means a reduction in NF. The high f_T, high β, and low r_b in aggressively scaled SiGe HBTs will enable low noise figure receiver design at increasingly higher frequencies. For LNA design, the transistor size can be optimized to make the noise matching resistance equal to the 50Ω source impedance. The 1/f noise factor K, which measures the amount of base current 1/f noise for a given base current, is independent of SiGe profile design. With scaling, the K factor and 1/f noise corner frequency increase [29, 50].

Noise figure can be determined with the following equation [50]:

$$\left(n_i^2\right)_{SiGe} = n_{io}^2 \exp\frac{\Delta E_G}{kT}\left[\frac{(N_C N_V)_{SiGe}}{(N_C N_V)_{Si}}\right] \qquad \textbf{(4.1)}$$

Where R_n is the noise resistance and C_i is;

$$C_i = {g_m}/{2\pi f_T} \qquad \textbf{(4.2)}$$

4.3 Proposed SiGe UWB LNA Circuit

This three staged amplifier which is designed in AMS0.35µ BiCMOS process promises -14dB input return loss and maximum gain 32.8dB with 3.3V supply. The circuit satisfy the 50Ω input matching along whole UWB band. Moreover, the operating band of this state of art low noise amplifier expands from 3.1GHz-10.6GHz to 1GHz-15GHz by applying optimization techniques.

The first stage of the LNA is a common-base amplifier in which the signal source and the load share the base of the transistor as a common connection point. Although, HBTs are almost exclusively operated in a common emitter configuration (CE) in amplifier design a common base configuration (CB) has the advantages of ease of broadband impedance matching with a better gain and is more suitable for optical and microwave broadband communication applications.

The topology of this stage is seen in Figure 4.2. c_i and r_i are the input capacitance and resistance of the second stage and they are considered as 75fF and 1.5KΩ. The passive elements R_{d1}, L_{d1}, R_{d2}, L_{d2}, C_1, C_2, L_3, L_4 and R_6 are added to the common base configuration to keep the input impedance at $1/g_{m1}$. R_5 is placed for biasing purpose. Q1 is biased in forward active region with the proper selection of R_5. The input impedance of Q1 aims to deviate from $1/g_{m1}$ as the frequency increases. The main idea is to eliminate these deviations in several regions by superposing the multiple resonances [45].

This circuit contains three multiple resonances which are placed to the low frequencies, middle frequencies and high frequencies of the band of interest. The proposed work was based on resonances on two different frequencies. On of them is near to lower edge and the second one is the near to higher edge of the UWB band [45]. The resonance in the mid frequencies in this circuit is one step further in optimisation and this makes the design unique.

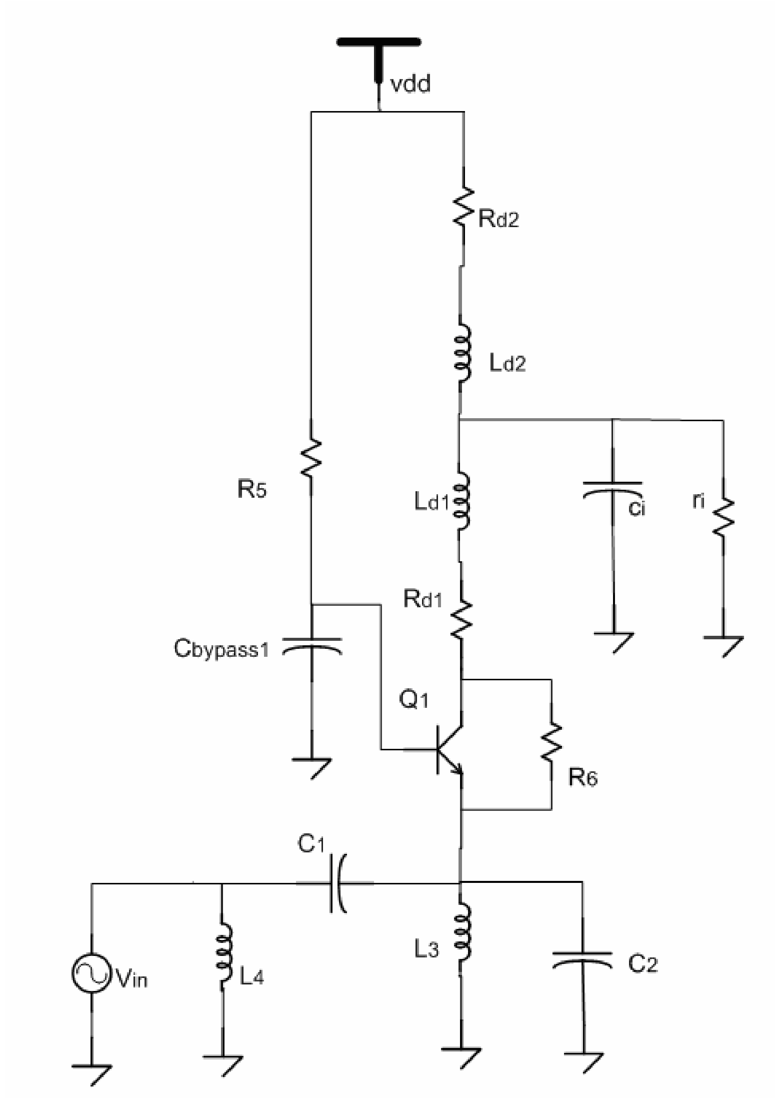

Figure 4.2 : Common-base input stage of LNA.

The Norton equivalent circuit can be sketched as Figure 4.3 where L_e and C_e are the parasitics in emitter of Q1.

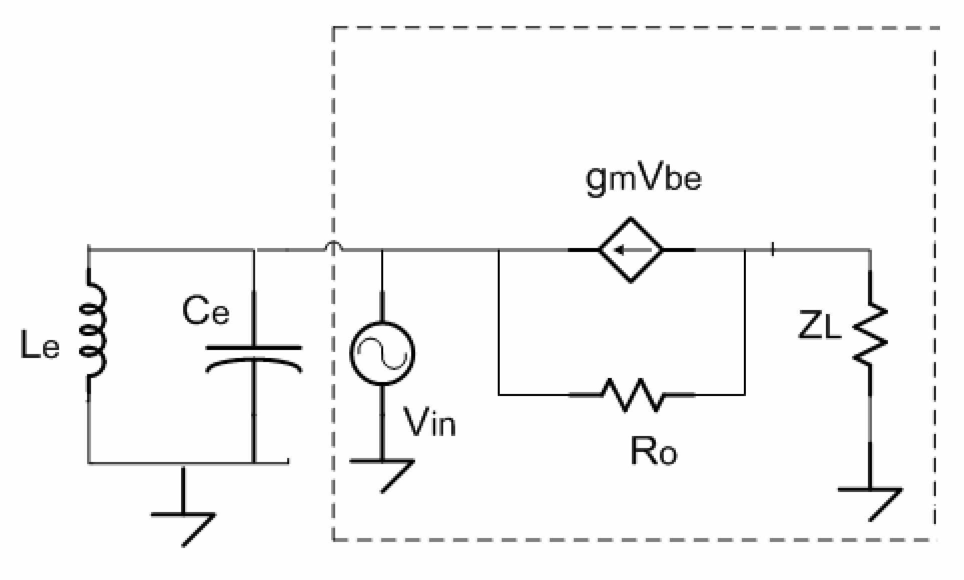

Figure 4.3 : Norton equivalent circuit of the first stage.

The parallel equivalence of L_e // C_e can ignored when they are high enough. By using this assumption, input impedance of the circuit can be derived with using Thevenin equivalent circuit.

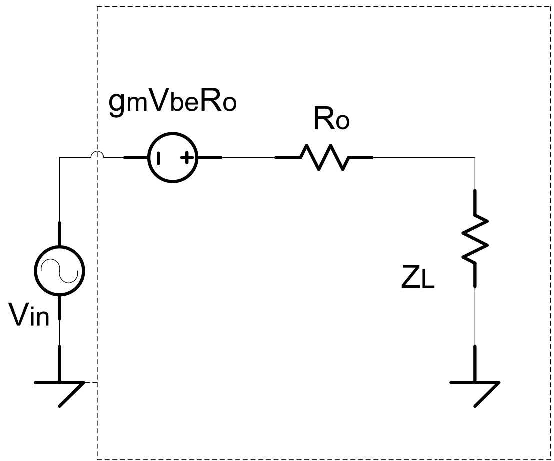

Figure 4.4 : Thevenin equivalent circuit of the first stage.

In Thevenin equivalent on Figure 4.3 where g_{m1} is the transconductance and R_0 is the output conductance of Q1:

$$V_{be} = -V_i \tag{4.3}$$

$$\frac{V_i - g_{m1}R_0V_i}{R_0 + Z_L} = I_i \tag{4.4}$$

$$\frac{V_i}{I_i} = \frac{R_0 + Z_L}{1 + g_{m1}R_0} \tag{4.5}$$

Hence $g_mR_0 >> 1$,

$$\frac{V_i}{I_i} = \frac{R_0 + Z_L}{g_{m1}R_0} \tag{4.6}$$

The last equation can be rearranged as follows:

$$Z_{in} = \frac{1}{g_{m1}}\left(1 + \frac{Z_L}{R_0}\right) \tag{4.7}$$

(4.5) is the starting point in the design flow of this circuit since the main requirement is providing 50Ω matching in the input which means Z_{in}=50Ω. Under the condition of $Z_L=R_0$, Z_{in} becomes:

$$Z_{in} = \frac{2}{g_{m1}} \tag{4.8}$$

g_{m1} has to be 40mS in order to set Z_{in} to 50Ω without deviating from $Z_L=R_0$.

This is a great advantage of common base topology in design challenge and can be enough to design a low noise amplifier for a single frequency. However with the increasing frequencies, it is obvious that some deviations are going to be occurred in this equation because of the effects of parasitic capacities in the emitter of Q1 which are ignored seen in Figure 4.3. These deviations degrade the performance.

This circuit should dynamically balance these deviations to kept the $Z_L=R_0$ condition. The goal is creating resonances in the points which this equation tends to deviate.

It has been thought before to satisfy UWB conditions by simultaneous resonances but this is the unique design that controls the performance by setting three resonances in different frequencies.

The resonances can be set around 1GHz, 5GHz and 10GHz to shift the performance up.

In Figure 4.5 the small signal equivalent circuit of the common-base circuit in Figure 4.2 is given. R_6 in Figure 4.2 dominates the r_{ce} in small signal circuit. In around 5GHz which is in middle part of the operating frequency range, R_{d1} and L_{d1} are low enough to neglect. $c_i//L_{d2}$ and $L_e//C_e$ pair resonate simultaneously by the proper choice of L values. R_{d2} is adjusted to keep $Z_L=R_0$. Placing C_2 and C_1 brings other resonance frequencies around 1GHz and 10GHz.

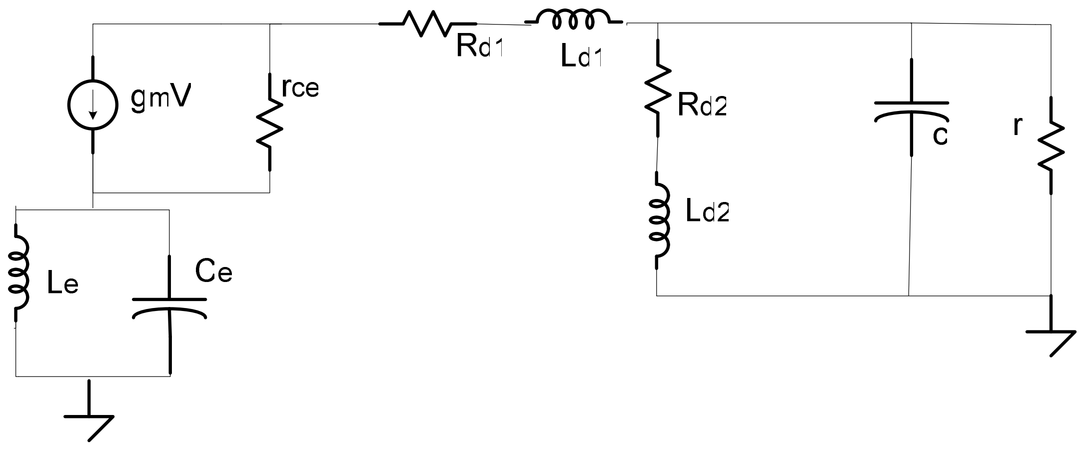

Figure 4.5 : Small signal equivalent of Figure 4.2.

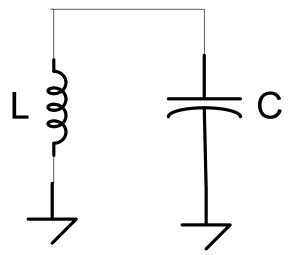

Figure 4.6 : Resonated L//C pair.

The parallel resonance in Figure 4.6 can be defined as follows:

$$f_{resonance} = \frac{1}{2\pi} \cdot \sqrt{\frac{1}{(CL)}} \quad \textbf{(4.9)}$$

Element values were determined using the equation in (4.9) and some parametric analysis. The simulation results verify the multiple resonance design goal. The matching is provided between 400MHz and 14GHz as seen in Figure 4.7.

The circuit is designed using Cadence® Virtuoso® Spectre Circuit Simulation program in ITU VLSI laboratories.

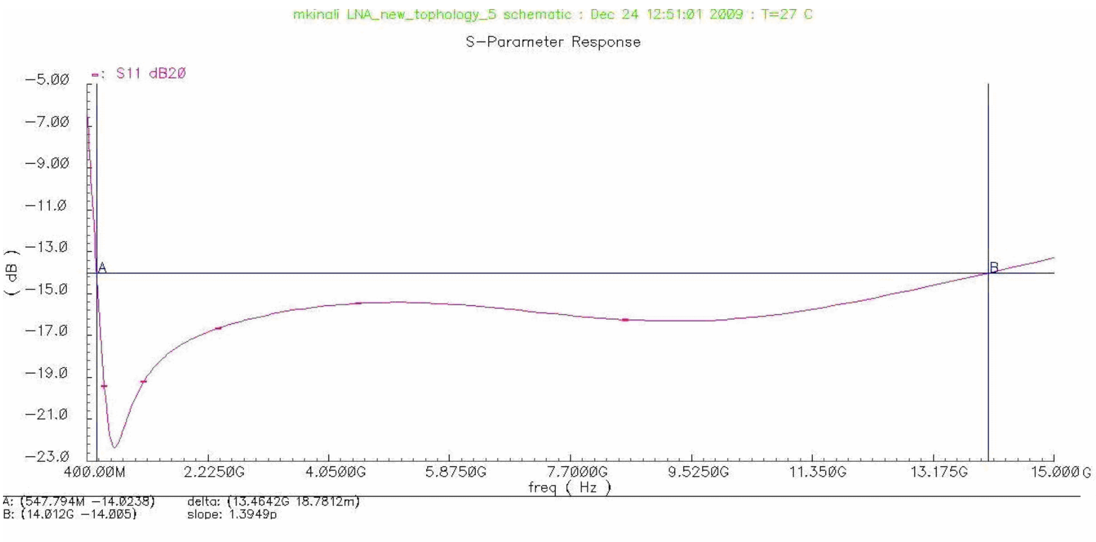

Figure 4.7 : Input return loss of the first stage.

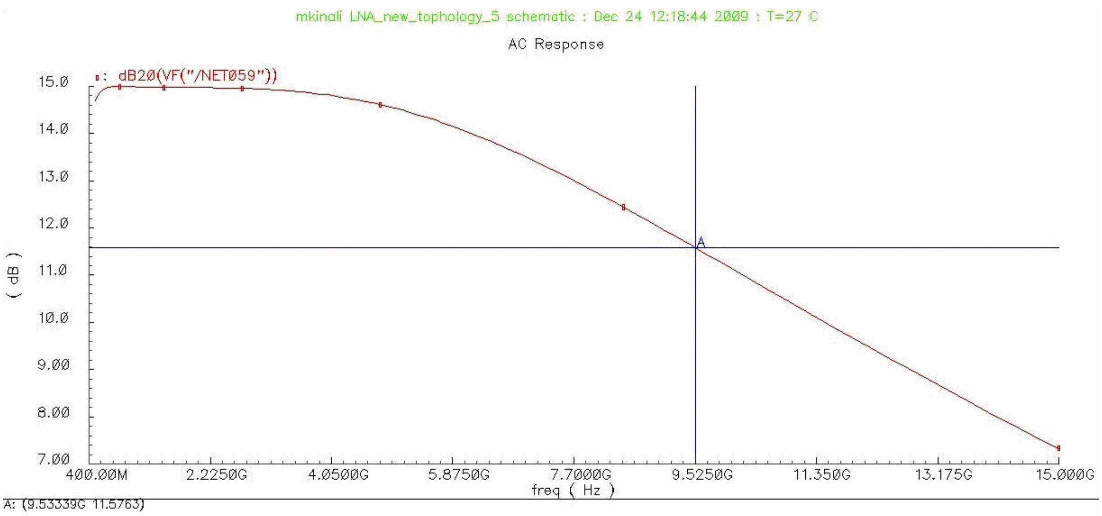

Figure 4.8 : Gain of the first stage.

The gain is seen in Figure 4.8. The decreasing gain level with increasing frequencies leads to place additional stages. Cascading with another stage can bring adequate signal amplification. Since S_{11} is determined with first stage, the following stages cannot degrade this characteristic. The noise figure of a multistage low noise amplifier is determined by the first stage. Q1 is key element in the noise characteristic. Figure 4.9 shows the NF of the circuit in Figure 4.2.

A following cascode configuration can pick up the drop in the performance but second stage is selected as an emitter follower topology because of its characteristic of high input resistance. The output of the first stage is designed according to the high output resistance. The last stage cannot be connected to the first stage without this common collector amplifier. The output voltage of a common-collector amplifier is always nearly equal to the input voltage. The emitter load voltages follow the input so closely. The DC level is tuned properly to keep Q2 in the forward active region. The node voltage at the base of Q2 is 1.8V. Thus additional bias is not required in this configuration.

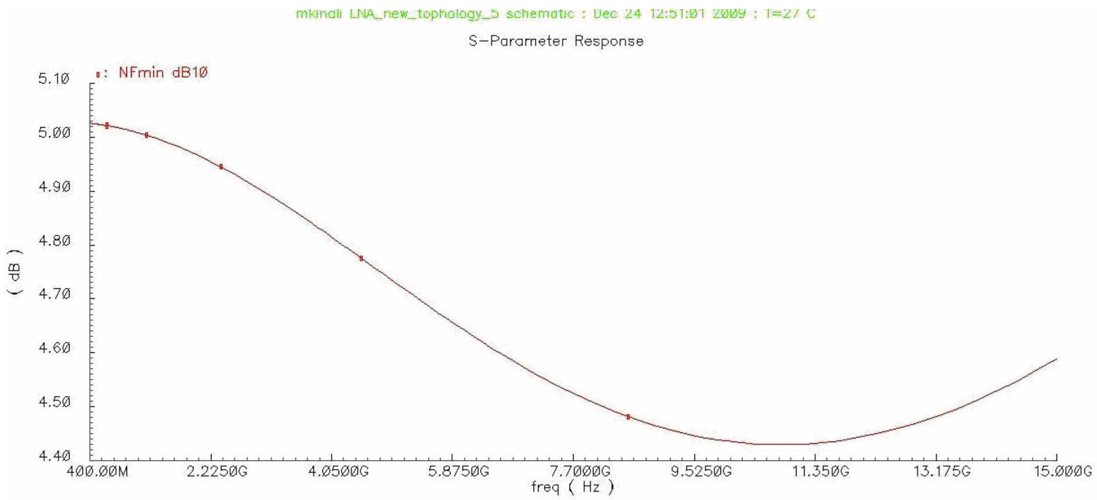

Figure 4.9 : Noise figure of the first stage.

The last stage is a compensated common emitter topology which contains some optimisation inductances and a shunt-series feedback. These optimisations bring inductive effects which are shifting up the gain level in frequencies above 8GHz. The stage consists of Q3 and Q4. The topology is given in Figure 4.10. R_{24} and R_{25} is placed for biasing. R_{21} is a resistive feedback. The tuning of these resistor values are challenging to provide the DC conditions.

The circuit in Figure 4.10 cannot satisfy the requirements as a last stage. This is obviously seen in the gain characteristic in Figure 4.11.

The additional inductors placed into the circuit to fix the problem which is seen in high frequencies. The inductive effects coming from L_{21}, L_{22}, L_{23} and L_{24} can shift up the gain level. Figure 4.12 is the new topology for the third stage.

The final performance metrics are given for the new common emitter architecture with the following graphs in Figure 4.13.

The own gain characteristic of the third stage is tuned to be cascaded with the following stages and the final topology of the LNA is given in Figure 4.14 after combining these three amplifier stages.

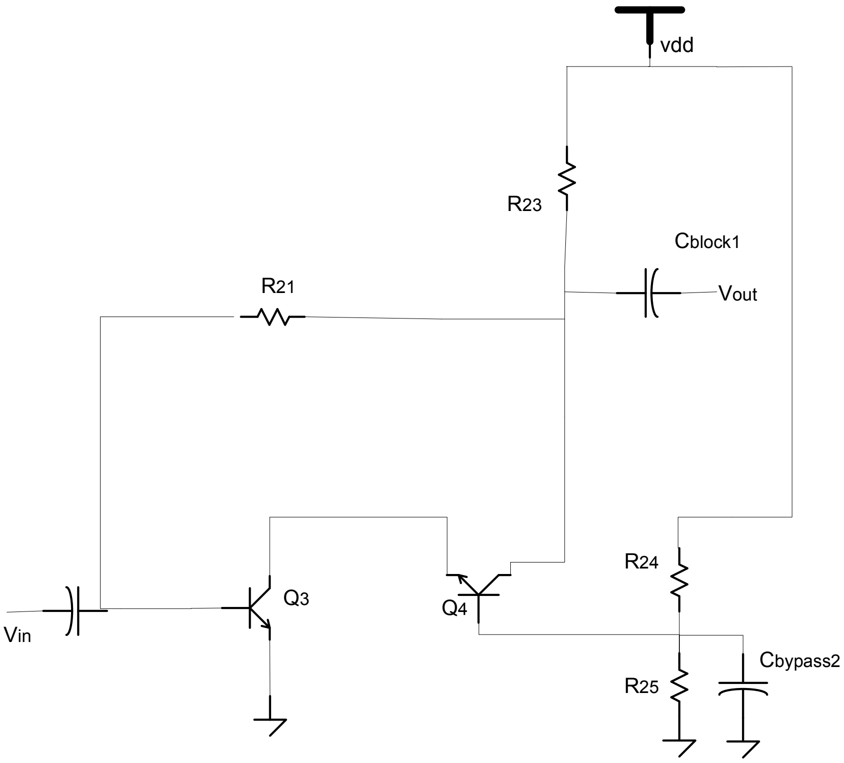

Figure 4.10 : Common emitter stage without compensation.

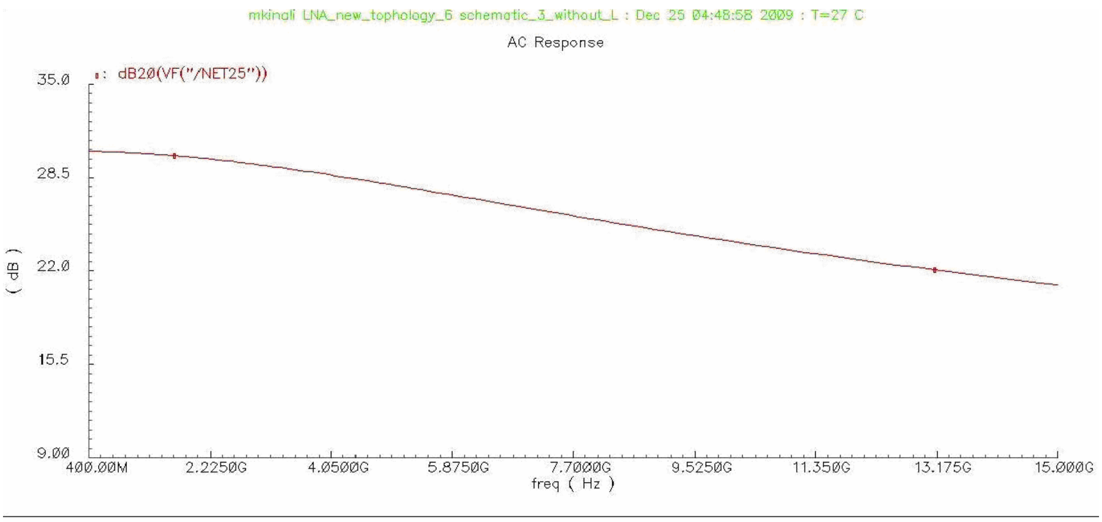

Figure 4.11 : Gain of the circuit in Figure 4.10.

The final topology of the proposed low noise amplifier circuit is seen in Figure 4.14. Its performance outputs is shown in the following graphs in Figure 4.15 and Figure 4.16 respectively.

The simulation results show there can be more improvement opportunity in the studied three staged amplifier. Firstly removing L_{d1} and R_{d1} decrease the number of the elements that are used in the circuit. In order the shifting up the inductive effect coming from the second stage, an inductance can be placed to the in the input of Q2. Also an additional inductance between Q3 and Q4 results to improvement as it absorbs the effect of the parasitic capacities in the emitter of Q3. In this configuration g_{m3} and g_{m4} becomes 26mS. The f_t of the transistors (Q1, Q2, Q3 and Q4) are around 60GHz.

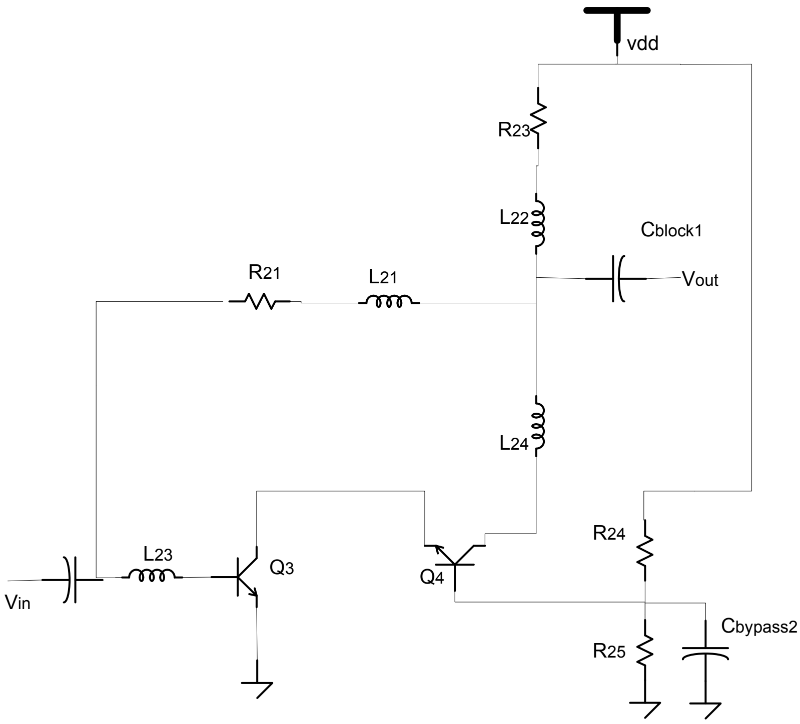

Figure 4.12 : Common emitter stage with compensation.

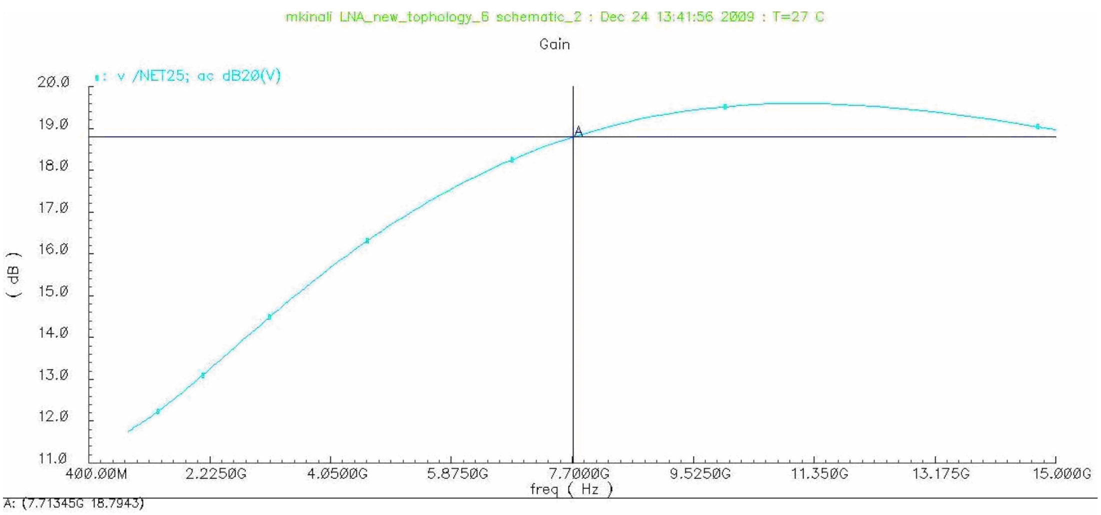

Figure 4.13 : Gain of the last stage.

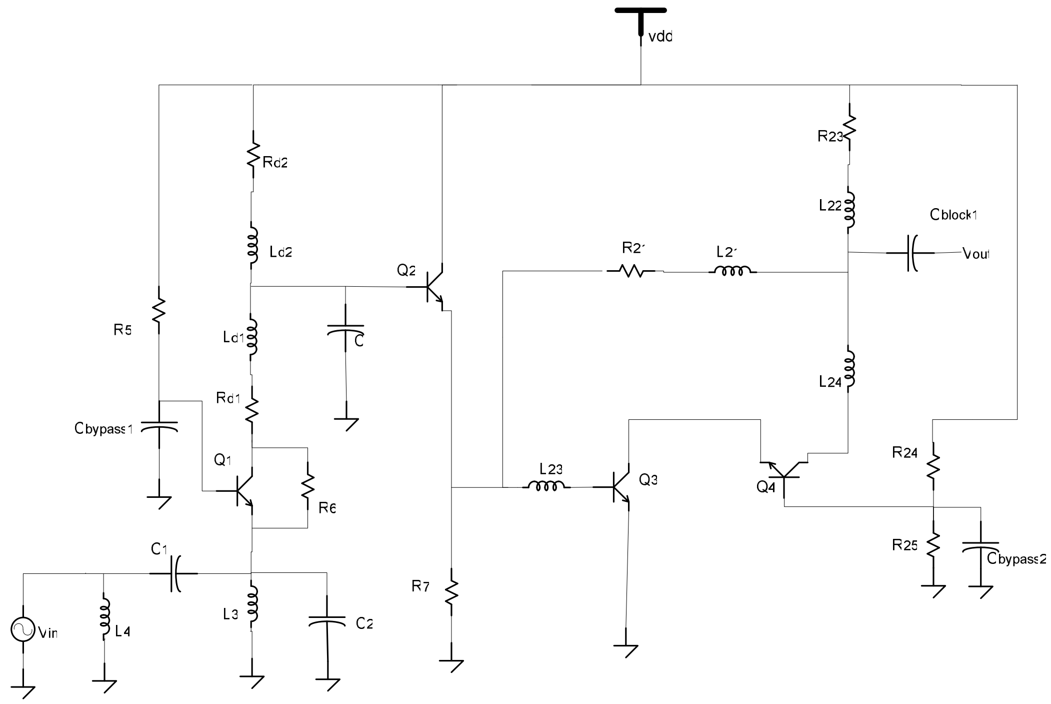

Figure 4.14 : Three staged state of art low noise amplifier.

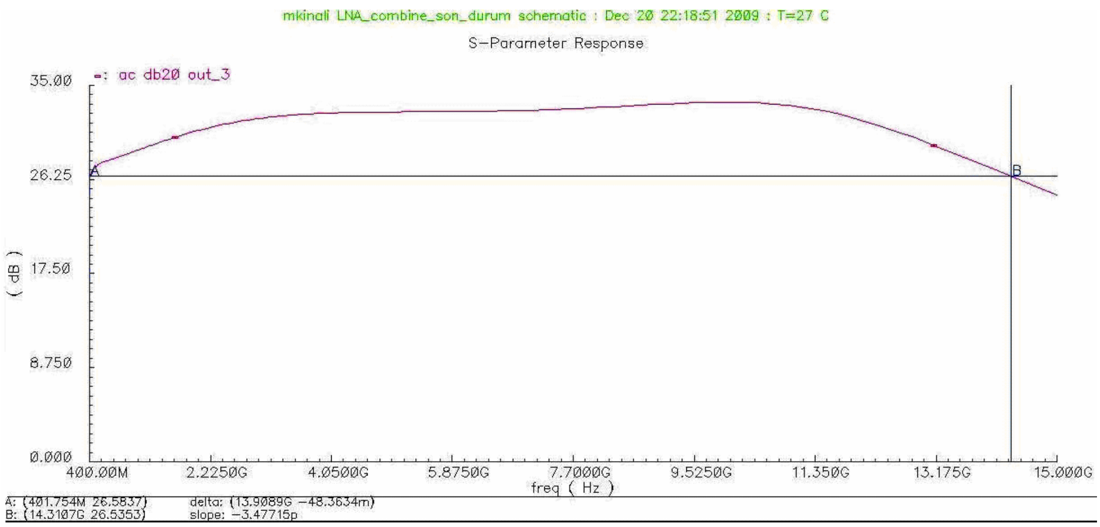

Figure 4.15 : Gain of the LNA.

The final version of circuit can be seen on the Figure 4.17. L_{c1} and L_{c2} are the last two elements which are added to the circuit. Figure 4.18 gives the S_{11} characteristic. There is not any degradation in S_{11} and it is lower than -14dB between 400MHz and 14GHz. The gain is around 32dB. The 3dB bandwidth is between 1.5GHz and 15GHz. The power dissipation is somewhat high. The source current is 7.8mA and the supply voltage is 3.3V which yields 29mW power consumption.

The element values are given in Table 4.1. The topology promises high voltage gain, low return loss over a wide band and a new architecture.

The comparasion of performance of this architecture with recent papers is given in Table 4.2. The benchmark contains different topologies and processes; CMOS, SiGe and HEMT. There are some trade-offs between some designs. Some of the works aim to dissipate power as minumum as possible. Some of them are designed under restrict noise figure condition. The proposed low noise amplifier in this study prserves best matching over the widest frequency range including 3.1-10.6GHz.

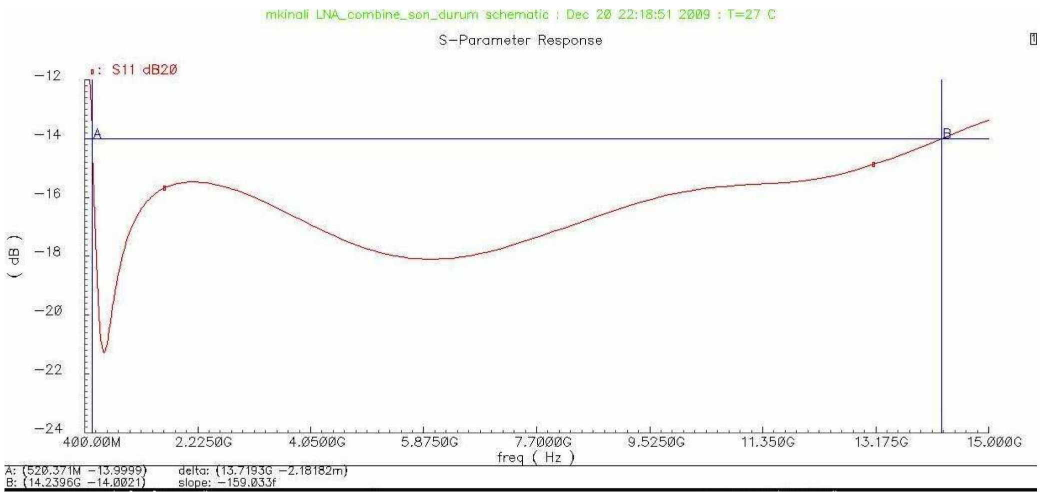

Figure 4.16 : Input return loss of the LNA.

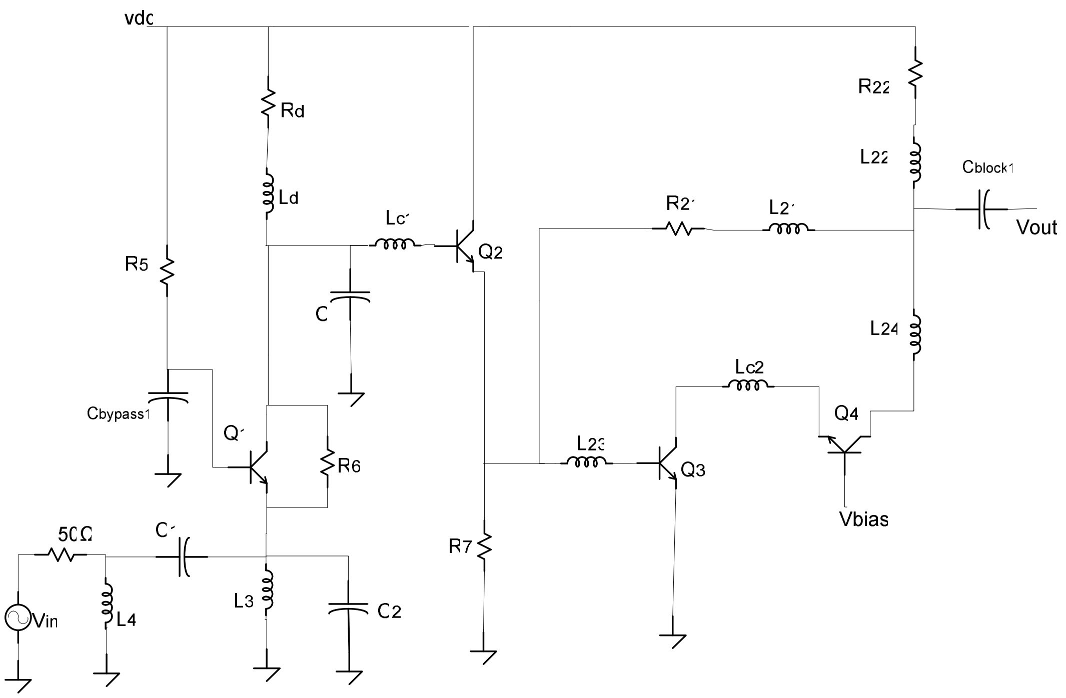

Figure 4.17 : The final schematic of the studied LNA architecture.

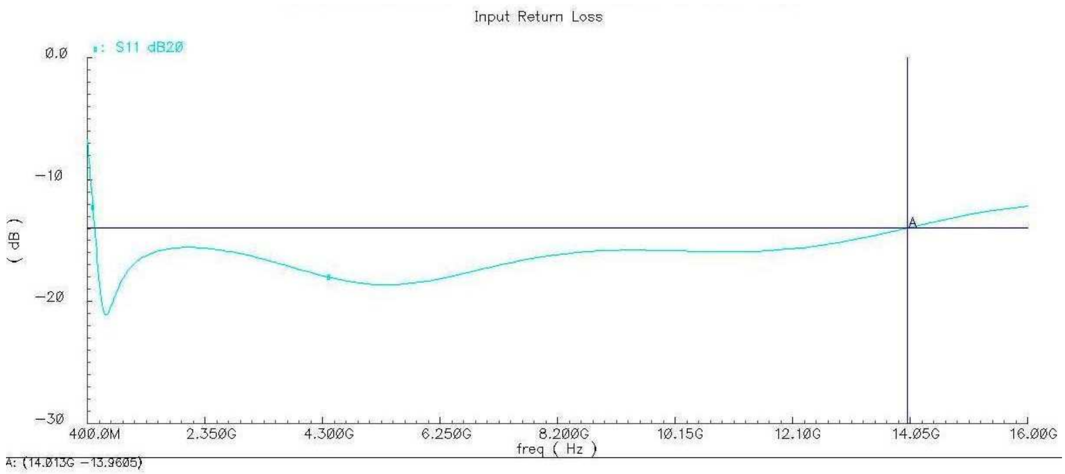

Figure 4.18 : Input return loss of the studied LNA circuit (last version).

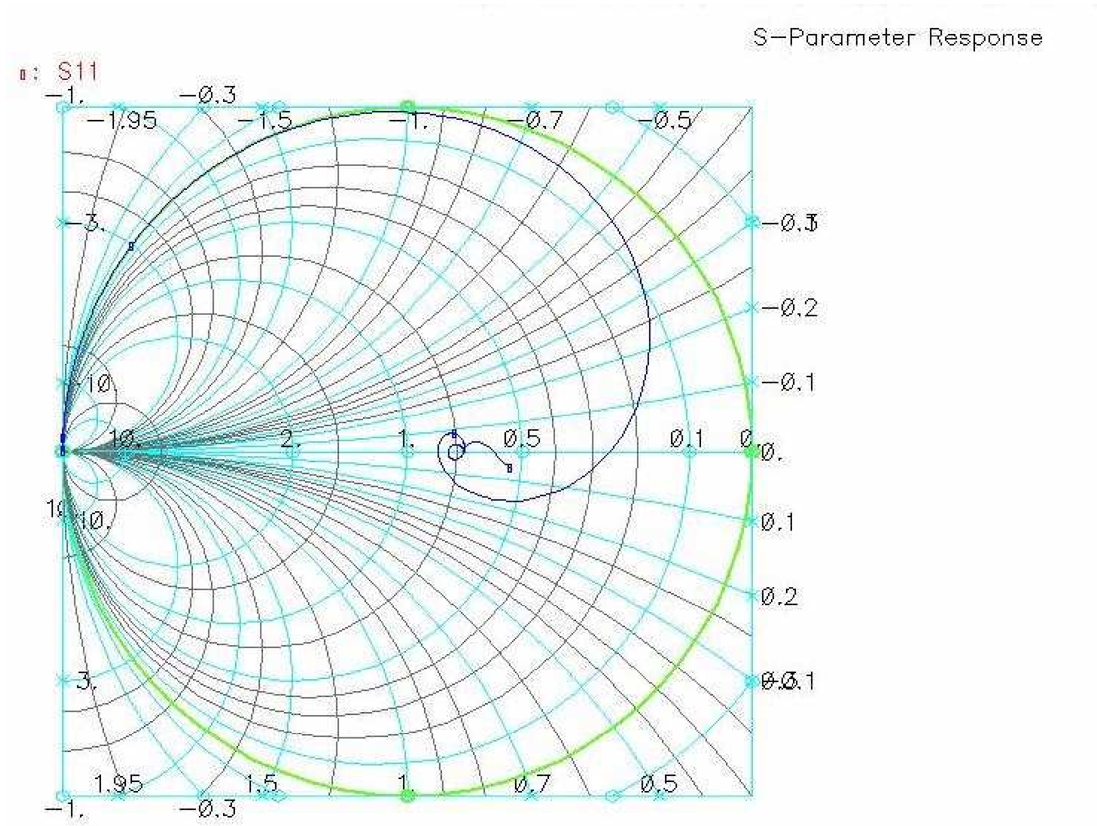

Figure 4.19 : Input return loss on Smith Chart (last version).

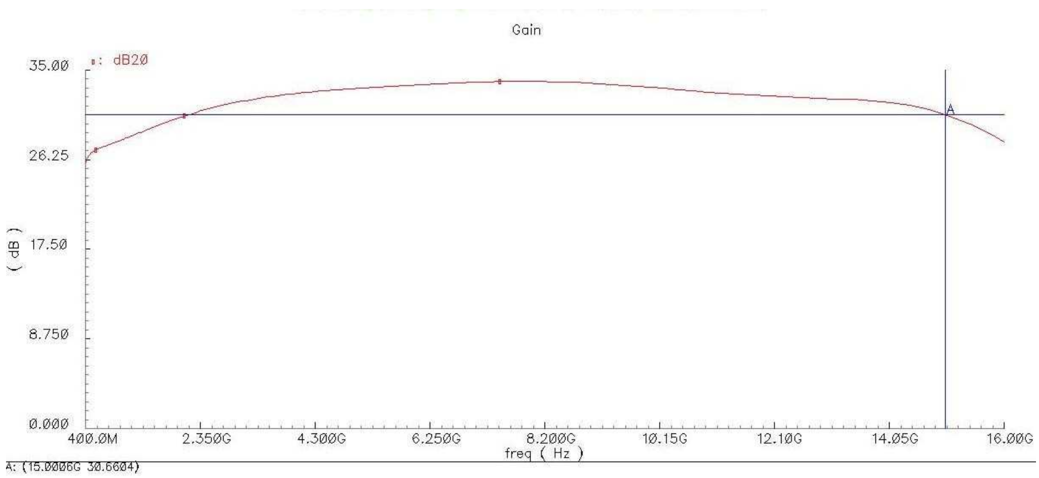

Figure 4.20 : Gain of the studied LNA circuit (last version).

Table 4.1: Element values in the studied circuit.

Elements	**Value**	**Elements**	**Value**
C_1	4.3pF	R_7	250Ω
C_2	60fF	L_{c1}	8nH
$C_{bypass1}$	50pF	L_{c2}	2nH
C_i	80fF	L_{21}	20nH
L_3	25nH	L_{22}	35nH
L_4	35nH	L_{23}	4nH
L_d	8nH	L_{24}	12nH
R_d	425Ω	R_{21}	1.1KΩ
R_5	400KΩ	R_{22}	315Ω
R_6	700Ω	C_{block1}	50pF

Table 4.2: Performance comparision of UWB LNA previously designed

Reference	[34]	[45]	[44]	[51]	[41]	This work
S_{11}	<-9.9dB	<-10dB	<-5dB	<-7.2dB	<-7dB	<-14dB
Gain	9.3dB	16dB	10dB	20.3dB	13dB	32dB
BW	2.3 - 9.2GHz	3 -11GHz	3-10GHz	0.1-13.6GHz	3.1-10.6GHz	1.2GHz - 15GHz
P_{DC}	9mW	9.54mW	NA	26mW	13.5mW	29mW
NF	<8.5dB	<4dB	<2.5dB	<3.1dB	<7.2dB	<10dB
Process	0.18µm CMOS	0.18µm CMOS	InAlAs/ InGaAs HEMTs	0.18 µm SiGe BiCMOS	0.35 µm SiGe BiCMOS	0.35 µm SiGe BiCMOS

5. UWB LOW NOISE AMPLIFIER DESIGN

Ultra-wideband technology becomes very popular recently. As 3.1-10.6GHz frequency band was allocated to UWBB in 2002 for unlicensed usage by FCC, the commercial applications started to employ UWB systems. Other related standards for UWB systems were preserved and new approaches were done. It is more suitable for the wireless personal area networks because it enables transfer high data rates in short distances. This makes UWB as an efficient solution not only for military applications as radar and weapon systems also for commercial applications such as PDAs, cell phones, pagers, game consoles, portable computing devices, body imaging and positioning devices.

Also from the radio frequency integrated circuit designers' point of view transreceiver architectures become less complex. Costs were reduced. But as the frequency range is huge the providing stability of the sub-blocks over the full of this range is a big problem. On the other hand UWB standards contain strong restricts especially for the power emissions. This brings new challenges to the UWB transreceiver design.

Although, CMOS technology dominates the microprocessor market, the wireless and high-data-rate wireline domains are another matter entirely, and place far more stringent demands on the devices than simple digital logic. SiGe is the new trend for to satisfy these demands as having superior radio frequency characteristics. UWB standardization and SiGe technology can meet in RF IC design.

LNA is the most important block in a for the narrowband and wideband transreceivers. Hence it is the first block its noise, gain and the stability characteristics should be excellent. LNA design becomes more difficult as the telecommunication industry started to demand ultra-wide band LNAs. Different than the narrowband topologies new techniques should be applied to keep the performance of the LNA over 7.5GHz range. Common-base topology becomes one step further as its matching and the stability characteristics are more suitable for UWB requirements.

In this work three staged UWB LNA circuit was designed for the first time with using AMS0.35µ BiCMOS process. The stages are common-base, common-collector and compensated cascode respectively. In the first stage multiple resonances are used to satisfy full band input matching and the cascode stage with a feedback fixes the gain characteristic by shifting up the level especially in high frequencies to satisfy the flatness. Its gain level and the flatness properties are very satisfying. The noise characteristic of the circuit should be optimized in one more step to be proper with UWB applications. The outputs are spectacular among the other recent studies.

As a further work, the performance of the first circuit is investigated to increase its noise performance. Some extra optimization methods can be applied to this circuit. Without degrading its excellent flatness a trade-off can be considered between gain level and noise figure.

Another possibility is changing the process such as 0.25µm to decrease the power dissipation and spend less area. Also, applying advanced layout techniques can increase the performances of the circuit. UWB has got plenty of advantages over narrow band systems.

REFERENCES

[1] **Safarian, A. and Heydari, P.** 2008. *Silicon-Based RF Front-Ends for Ultra Wideband Radios*, Springer.

[2] **Ghavami, M., Michael, L. B., Kohno, R.,** 2004. *Ultra Wideband Signals and Systems in Communication Engineering*, John Wiley & Sons Ltd.

[3] **Nekoogar, F.,** 2005. *Ultra-Wideband Communications: Fundamentals and Applications*, Prentice Hall.

[4] **Aiello, R. G. and Rogerson, G. D.,** 2003. Ultra-Wideband Wireless Systems, *IEEE Microwave Magazine,* **June**, pp. 37-47.

[5] **FCC 02-48,** 2002. First report and order, *Federal Communications Commission,* Washington.

[6] **Nikookar H., Prasad, R.** 2009. *Introduction to Ultra Wideband for Wireless Communications*, Springer.

[7] **Kissick, A. W.**, 2001. The temporal and spectral characteristics of ultrawideband signals, *U.S Department of Commerce NTIA Report,* **NTIA Report 01-383,** U.S Department of Commerce, USA.

[8] **Molisch, F. A., Foerster, R. J., and Pendergrass, M.,** 2003. Channel Models for Ultrawideband Personal Area Networks, *IEEE Wireless Comm.,* December, pp. 14-21

[9] **Lu, Y., Seng, K., Cabuk, A., Ma, J., Do, A. M., and Lu, Z.,** 2006. A Novel CMOS Low-Noise Amplifier Design for 3.1 to 10.6-GHz Ultra-Wide-Band Wireless Receivers, *IEEE Trans. Circuits and Systems*, 53, pp. 1683-1692.

[10] **Aiello, R. G.,** 2003. Challenges for Ultra-Wideband (UWB) CMOS Integration, *IEEE MTT-S Digest,* pp. 361-364.

[11] **Barras, D., Ellinger, F., and Jäckel, H.,** 2002. A Comparison between Ultra-Wide-band and Narrow-band Transceivers, *TRLabs/IEEE Wireless*, July, pp. 211-214.

[12] **Harald, I., and Lüth, H.,** 1996. *Solid-State Physics, An Introduction to Principles of Materials Science (Second ed.)*, Springer-Verlag.

[13] **Ashburn, P.,** 2003. *SiGe Heterojunction Bipolar Transistors*, John Wiley & Sons Ltd.

[14] **Cressler, J. D., and Niu G.,** 2003. *Silicon-Germanium Heterojunction Bipolar Transistors*, Artech House INC.

[15] **Kasper, E., and Paul D. J.,** 2005. *Silicon Quantum Integrated Circuits*, Springer.

[16] **Zeghbroeck, V. B.,** 2008. *Principles of Semiconductor Devices and Heterojunctions*, Prentice Hall Ptr.

[17] **Ruzyllo, J.,** 2004. *Semiconductor Glossary; An introduction to Semiconductor Terminology*, Prosto Multimedia Publishing.

[18] **Yu, Y. P., and Cardona, M.,** 2005. *Fundamentals of Semiconductors; Physics, and Material Properties*, Springer.

[19] **Capasso, F.,** 1987. Band-Gap Engineering: From Physics and Materials to New Semiconductor Devices, *Science*, Vol. **235**. No. 4785, pp. 172 – 176.

[20] **Rieh, S. J. et all,** 2002. SiGe HBTs with Cut-off Frequency of 350 GHz, *IEDM Technical Digest*, 2002, pp.771-774.

[21] **Alamo, D. J., Swirhun S., and Swanson M. R.,** 1986. Simultaneous Measurement of Hole Lifetime, Hole Mobility, and Bandgap Narrowing in Heavily Doped n-type Silicon, *IEDM Technical Digest*, 1986, pp. 290-293.

[22] **Swirhun, E. S., Kwark, H. Y., and Swanson, M. R.,** 1987. Measurement of Electron Lifetime, Electron Mobility, and Bandgap Narrowing in Heavily Doped p-type Silicon, *IEDM Technical Digest*, 1987, pp.24-27.

[23] **Jeng, J. S. et al.,** 2001. A 210-GHz *fT* SiGe HBT with Non-self-aligned Structure, *IEEE Elect. Dev. Lett.*, vol. **22**, pp. 542-544.

[24] **Joseph, J. A. et al.,** 2002. 0.13 μm 210 GHz *fT* SiGe HBTs - Expanding the Horizons of SiGe BiCMOS, *Tech. Dig. IEEE Int. Solid-State Circ. Conf. 2002*, pp.180-182.

[25] AMCC S2090CB preliminary data, http://www.amcc.com, accessed 2002.

[26] AMCC S4803 preliminary data (http://www.amcc.com), accessed 2002.

[27] **Saunders, D. et al.,** 2009. A single-chip 24 GHz SiGe BiCMOS Transceiver for FMCW Automotive Radars, 2009 IEEE Radio Frequency Integrated Circuits Symposium, IEEE, USA, 7-9 June, pp. 459-462.

[28] **Kasper, E., and Lyutovich, K.,** 2000. *Properties of Silicon Germanium and SiGe:Carbon*. INSPEC.

[29] **Pawlikiewicz, H. A., and El Rai E. S.,** 2007. RF CMOS or SiGe BiCMOS in RF and Mixed Signal Circuit Design, MIXDES 2007 International Conferance, IEEE, Polland, 21-23 June, pp 333-338.

[30] **Racanelli, M., and Kempf P.,** 2003. SiGe BiCMOS Technology for Communication Products, 2003 Custom Integrated Circuits Conference, IEEE, USA 21- 24 September, pp.331-334.

[31] **Li, X., et al.,** 2001. A comparison of CMOS and SiGe LNA's and Mixers for Wireless LAN Application**,** 2001 Custom Integrated Circuits Conference, IEEE, USA 6-9 May, pp. 531-534.

[32] **Razavi, B.,** 1998. *RF Microelectronics*, Prentice Hall Ptr.

[33] **Allstot, J. D., Xiaoyong, Li, and Shekhar, S.,** 2004. Design Considerations for CMOS Low-Noise Amplifiers, 2004 IEEE Radio Frequency Integrated Circuits Symposium, IEEE, USA, 6-8 June, pp.97-100.

[34] **Bevilacqua, A., and Niknejad, M.,** 2004. An Ultrawideband CMOS Low-noise Amplifier for 3.1-10.6 GHz Wireless Receivers, *IEEE Journal of Solid State Circuits*, Vol. **39**, pp.2259-2268

[35] **Fan, X., Sinencio, S. E., and Martinez, S. J,** 2005. A 3GHz-10GHz Common Gate Ultrawideband Low Noise Amplifier, 48th Midwest Symposium on Circuits and Systems, IEEE, USA, 7-10 August, pp. 631-634.

[36] **Taris, T., Begueret, J. B., and Deval, Y.,** 2007. A Low Voltage Current Reuse LNA in a 130nm CMOS Technology for UWB Applications, 2nd European Microwave Integrated Circuits Conference, IEEE, Munich, 9-12 October, pp. 307-310.

[37] **Yu, H. Y., Chen, E., and Heo, D.,** 2006. An Ultra-low Voltage UWB CMOS Low Noise Amplifier, Asia-Pacific Microwave Conference 2006, IEEE, Japan, 12-15 December, pp. 313-316.

[38] **Barras, D. et al.,** 2004. A Low Supply Voltage SiGe LNA for Ultra-Wideband Frontends. *IEEE Microwave and Wireless Comp. Let.,* **14,** pp 469-471

[39] **Yunseo, P. et al.,** 2006. Theoretical Analysis of a Low Dispersion SiGe LNA for Ultra-wideband Applications, *IEEE Microwave and Wireless Comp. Let.,* **16,** pp 517-519

[40] **Pei, S. et al.,** 2008. An Ultra-Wideband Darlington Low Noise Amplifier Design Based on SiGe HBT, ICMMT 2008, IEEE, USA, 21-24 April, pp. 1372-1375.

[41] **Tsai, M.-D., Lin., K.-Y., and Wang, H.,** 2005. A 5.4-mW LNA Using 0.35-pm SiGe BiCMOS Technology for 3.1-10.6-GHz UWB Wireless Receivers, *Radio* Frequency Integrated Circuits Symposium 2005, IEEE, USA, 12-14 June, pp. 335-338.

[42] **Zi-xu, W. et al.,** 2008. The Design of SiGe HBT Balanced Broadband Low Noise Amplifier, International Conference on Microwave and Millimeter Wave Technology 2008, IEEE, China, 21-24 April, pp. 233-236.

[43] **Seo, S., Pavlidis, D., and Moon, J.,** 2005. A Wideband Balanced AlGaN/GaN HEMT MMIC Low Noise Amplifier for Transceiver Front-ends, 13th Gallium Arsenide and Other Semiconductor Application Symposium, IEEE, Paris, 3-4 October, pp. 225-228.

[44] **Yoo, C. et al.,** 2008. A Ultrawideband Low Noise Amplifier Using Metamorphic HEMT on Organic Substrate, *Asia-Pacific Microwave Conference 2008,* IEEE, Hong Kong, 16-20 December, pp. 1-4.

[45] **Shim, Y., and Kim, C. W.,** 2007. Design of Full Band UWB Common-Gate LNA, *IEEE Microwave and Wireless Comp. Let.,* **17,** pp. 721-723.

[46] **Shiramizu, N. et al.,** 2005. A 3-10 GHz Bandwidth Low-Noise and Low-Power Amplifier for Full-Band UWB Communications in 0.25-μm SiGe BiCMOS Technology, Proccedings of RFIC Symphosium 2005, IEEE, USA, 12-14 June, pp. 39-42.

[47] **Yen S. H. and Lin Y. S.,** 2006. Design and Implementation of a 1.2-to-17GHz UWB SiGe LNA with a Peaking Inductor, VLSI Design, Automation

and Test, 2006 International Symposium, IEEE, USA, 26-28 April, pp.1-2.

[48] **Ma, Z., et al.,** 2006. An omni-directional comparison between common-emitter and common-base SiGe HBTs**,** 8th International Conference on Solid-State and Integrated Circuit Technology, IEEE, China, 23-26 October, pp.166-169.

[49] **Qin. G., et al.,** 2006. SiGe HBT Linearity Comparison Between CE and CB Configurations, 3rd International SiGe Technology and Device Meeting, IEEE, USA, 15-17 May, pp.1-2.

[50] **Niu, G.,** 2005. Noise in SiGe HBT RF Technology: Physics, Modeling, and Circuit Implications, *Proceedings of the IEEE,* Vol. **93**. Issue.9, pp. 1583 – 1597.

[51] **Lu, Y. et al.,** 2006. A 1.8-3.1 dB Noie Figure (3-10GHz) SiGe HBT for UWB Applications, 2006 Radio Frequency Integrated Circuits (RFIC) Symposium, IEEE, USA, 11-13 June, 4 pp.

CURRICULUM VITA

Candidate's full name: Murat KINALI

Place and date of birth: Elazığ, 24.06.1983

Permanent Address: Bağlarbaşı M. İlke Sitesi No:C-4 Darıca/KOCAELİ

Universities and
Colleges attended: **2001-2005: BSc. Program in Electronics Engineering, Istanbul Technical University.**